Rare decay modes of the K mesons in gauge theories

M. K. Gaillard* and Benjamin W. Lee†
National Accelerator Laboratory, Batavia, Illinois 60510‡
(Received 4 March 1974)

Rare decay modes of the kaons such as $K \to \mu\bar{\mu}$, $K \to \pi\nu\bar{\nu}$, $K \to \gamma\gamma$, $K \to \pi\gamma\gamma$, and $K \to \pi e\bar{e}$ are of theoretical interest since here we are observing higher-order weak and electromagnetic interactions. Recent advances in unified gauge theories of weak and electromagnetic interactions allow in principle unambiguous and finite predictions for these processes. The above processes, which are "induced" $|\Delta S| = 1$ transitions, are a good testing ground for the cancellation mechanism first invented by Glashow, Iliopoulos, and Maiani (GIM) in order to banish $|\Delta S| = 1$ neutral currents. The experimental suppression of $K_L \to \mu\bar{\mu}$ and nonsuppression of $K_L \to \gamma\gamma$ must find a natural explanation in the GIM mechanism which makes use of extra quark(s). The procedure we follow is the following: We deduce the effective interaction Lagrangian for $\lambda + \mathfrak{N} \to l + \bar{l}$ and $\lambda + \bar{\mathfrak{N}} \to \gamma + \gamma$ in the free-quark model; then the appropriate matrix elements of these operators between hadronic states are evaluated with the aid of the principles of conserved vector current and partially conserved axial-vector current. We focus our attention on the Weinberg-Salam model. In this model, $K \to \mu\bar{\mu}$ is suppressed due to a fortuitous cancellation. To explain the small K_L-K_S mass difference and nonsuppression of $K_L \to \gamma\gamma$, it is found necessary to assume $m_{\mathcal{P}}/m_{\mathcal{P}'} \ll 1$, where $m_{\mathcal{P}}$ is the mass of the proton quark and $m_{\mathcal{P}'}$ the mass of the charmed quark, and $m_{\mathcal{P}'} < 5$ GeV. We present a phenomenological argument which indicates that the average mass of charmed pseudoscalar states lies below 10 GeV. The effective interactions so constructed are then used to estimate the rates of other processes. Some of the results are the following: $K_S \to \gamma\gamma$ is suppressed; $K_S \to \pi\gamma\gamma$ proceeds at a normal rate, but $K_L \to \pi\gamma\gamma$ is suppressed; $K_L \to \pi\nu\bar{\nu}$ is very much forbidden, and $K^+ \to \pi^+\nu\bar{\nu}$ occurs with the branching ratio of $\sim 10^{-10}$; $K^+ \to \pi^+ e\bar{e}$ has the branching ratio of $\sim 10^{-6}$, which is comparable to the presently available experimental upper bound. The predictions of other models are briefly discussed. Relevant renormalization procedures and computational details are discussed in appendixes.

I. INTRODUCTION

Recent developments[1] in the study of spontaneously broken gauge invariance have led to the possibility of a unified and renormalizable theory of weak and electromagnetic interactions. Most such theories necessitate the introduction of weakly coupled neutral currents, and their viability depends on their success in accounting for the observed suppression of $|\Delta S| = 1$, $|\Delta Q| = 0$ semileptonic decays. In nearly all models proposed thus far, this problem is dealt with by appealing to the Glashow-Iliopoulos-Maiani (GIM) mechanism,[2] which we shall briefly recall.

A criterion for renormalizability is that couplings be invariant under a group of gauge transformations. The charged Cabibbo currents, $J_\mu^\pm$, together with the neutral current J_μ^3 defined by

$$J_\mu^3(x)\,\delta^4(x-y) = \tfrac{1}{2}[J_\mu^+(x), J_0^-(y)]\,\delta(x_0 - y_0) + \text{Schwinger terms} \qquad (1.1)$$

satisfy the algebra of SU(2). In a gauge-invariant theory these currents must couple with equal strength to gauge bosons. However, if $J_\mu^\pm$ are the usual Cabibbo current operators, the neutral current defined in Eq. (1.1) contains a strangeness-changing hadronic part as well as a leptonic part. The gauge-invariant coupling then implies that a decay such as $K_L \to \mu\mu$ should occur with a strength comparable to $K^+ \to \mu\nu$.

In the Weinberg-Salam model,[3] the remedy to this unwanted prediction is to modify the usual current

$$J_\mu^{c+} = \bar{\mathcal{P}}\gamma_\mu(1-\gamma_5)(\mathfrak{N}\cos\theta + \lambda\sin\theta) \qquad (1.2)$$

by adding a coupling

$$J_\mu^{+} = J_\mu^{c+} + \bar{\mathcal{P}}'\gamma_\mu(1-\gamma_5)(\lambda\cos\theta - \mathfrak{N}\sin\theta)\,, \qquad (1.3)$$

where θ is the Cabibbo angle; $\mathcal{P}$, $\mathfrak{N}$, and λ are the usual quarks and $\mathcal{P}'$ is a charmed quark with the charge of the proton quark. With this modification the current defined in (1.1) has no $|\Delta S| = 1$ component. It is generally assumed that $\mathcal{P}'$ is much heavier than the other quarks to account for the fact that charmed particles have not been observed.

In the Weinberg-Salam model the electromagnetic current is included by extending the gauge group to SU(2)×U(1); other constructions which satisfy low-energy phenomenology have also been proposed. For example, in the Georgi-Glashow model[4] the Cabibbo currents are modified by the

introduction of new particles in such a way that J_μ^3 is just the electromagnetic current and no other neutral current need be introduced. However, when higher-order processes are considered, an analog of the GIM mechanism must be used in all models of this type—increasing still further the number of quarks.

Rare decay modes of K mesons, such as $K_L \to \mu\bar{\mu}$ or $K_L \to \gamma\gamma$, are of immense theoretical interest because here we are dealing with the workings of higher-order weak and electromagnetic interactions; and a renormalizable theory of weak interactions provides in principle unambiguous and finite predictions for these decays. There is a general problem associated with higher-order transitions and it arises in the following way. The coupling constant g for charged bosons is comparable in strength to the electromagnetic coupling e. In the low-energy limit, where the boson propagator reduces to m_W^{-2}, first-order transitions are effectively governed by the Fermi constant

$$G_F/\sqrt{2} \sim g^2/m_W^2 \ .$$

For second-order processes, however, massive virtual bosons can be exchanged and the effective second-order coupling strength is found to be

$$g^4/m_W^2 \sim G_F \alpha \ .$$

Empirically, the strength of second-order processes involving a change of strangeness is characterized by $G_F^2\Lambda^2 \simeq G_F\alpha(\Lambda^2/m_W^2)$, where Λ is typically of the order of several GeV, as for the K_L-K_S mass difference and the decay $K_L \to \mu\bar{\mu}$. A mechanism is thus required to suppress the contribution of order $G_F\alpha$.

Consider, for example, the decays

$$K_L \to \gamma\gamma \ , \tag{1.4}$$

$$K_L \to \mu\bar{\mu} \ . \tag{1.5}$$

Diagrams contributing to the decay amplitudes are shown in Fig. 1. Setting $g \simeq e$ as is the case in unified theories of weak and electromagnetic interactions, both amplitudes are fourth order in the coupling e. Since the Feynman integrals are convergent, and since m_W is the dominant mass occurring in the propagators, each graph will give a factor m_W^{-2}. Then by virtue of the above discussion the two amplitudes will be of comparable strength:

$$\mathcal{A} \sim \frac{e^4}{m_W^2} \sim G_F\alpha \ . \tag{1.6}$$

Experimentally the decay rates are related by[5,6]

$$\Gamma(K_L \to \mu\bar{\mu}) \approx 2\times10^{-5}\Gamma(K_L \to \gamma\gamma)$$
$$\approx 4\times10^{-9}\Gamma(K^+ \to \bar{\mu}\nu) \ . \tag{1.7}$$

As expected, the amplitude for (1.4) is suppressed by roughly a factor α with respect to the first-order process $K^+ \to \mu\nu$. However, (1.5) is suppressed in amplitude by a factor of

$$\alpha^2 \approx 5M_p^2 G_F \ .$$

In fact a major contribution to the decay rate for (1.5) is from the higher-order electromagnetic process shown in Fig. 2. The imaginary part of the amplitude is dominated by the graph of Fig. 2 with the two photons on their mass shell; this contribution may be calculated in terms of the on shell $K_L \to \gamma\gamma$ coupling and is found to be[7]

$$\Gamma(K_L \to \mu\mu)_{\text{absorptive}} = 1.2\times10^{-5}\Gamma(K_L \to \gamma\gamma) \ . \tag{1.8}$$

The rate (1.8) is known as the "unitarity bound" for $K_L \to \mu\mu$, as it provides a lower limit for the partial width:

$$\Gamma(K_L \to \mu\mu) \geq \Gamma(K_L \to \mu\mu)_{\text{absorptive}} \ .$$

Thus a mechanism is required which suppresses the rate for $K_L \to \mu\mu$ to the experimentally observed level, and which leaves the rate for $K_L \to \gamma\gamma$ essentially unaffected. The role of the GIM mechanism is illustrated in Fig. 3. As the product of coupling constants [Eq. (1.3)] which enter in the virtual transition

$$\mathfrak{N} \to \mathcal{P}' + W^-$$
$$\searrow \ \lambda + W^+$$

is equal in magnitude and opposite in sign with respect to the similar process involving the $\mathcal{P}$ [Eq. (1.2)], the graph of Fig. 3(a) will exactly cancel the graph of Fig. 1(a) in the limit of equal $\mathcal{P}$ and $\mathcal{P}'$ masses. However, in the same limit the graph of Fig. 3(b) will also cancel the graph of Fig. 1(b), which is clearly not a desired result.

The problem can be posed most acutely in terms of symmetry properties. In the Weinberg-Salam model (as modified by GIM), the quarks transform

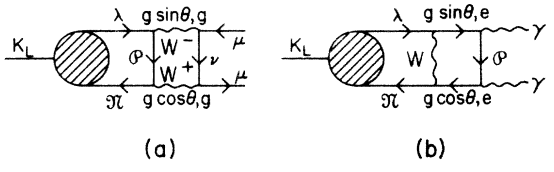

FIG. 1. Important diagrams for (a) $K_L \to \mu\bar{\mu}$ and (b) $K_L \to \gamma\gamma$.

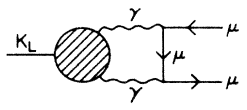

FIG. 2. Diagram which contributes to the absorptive part of the $K_L \to \mu\bar{\mu}$ amplitude.

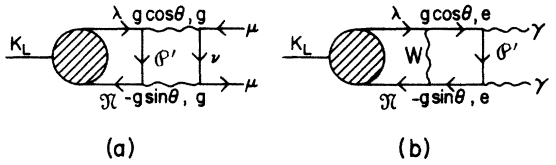

FIG. 3. Diagrams with the $\mathcal{P}'$-quark line which suppress the contributions of the diagrams in Fig. 1.

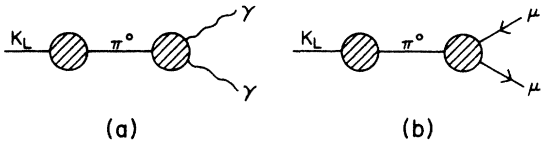

FIG. 4. Pole diagrams for (a) $K_L \to \gamma\gamma$ and (b) $K_L \to \mu\bar{\mu}$.

according to the fundamental representation of SU(4), with components $(\mathcal{P}', \mathcal{P}, \mathfrak{N}, \lambda)$. In analogy with I spin, which mixes $\mathcal{P}$ and $\mathfrak{N}$, or U spin, which mixes $\mathfrak{N}$ and λ, there is an SU(2) subgroup of SU(4) which mixes $\mathcal{P}$ and $\mathcal{P}'$. Let us call this group of transformations P spin. Then in the limit of $\mathcal{P}$ and $\mathcal{P}'$ degeneracy P spin is a symmetry of the strong interactions. The electromagnetic current is a P-spin invariant. The lowest-order hadronic operator with $\Delta Q = 0$ and $|\Delta S| \neq 0$ which can be constructed from the current of Eq. (1.3) is of the form

$$\sin\theta\cos\theta\ \bar{\mathfrak{N}}\ \lambda(\bar{\mathcal{P}}\mathcal{P} - \bar{\mathcal{P}}'\mathcal{P}') + \text{H.c.} + \text{charm-changing components.} \quad (1.9)$$

The operator (1.9) is a P-spin vector; that is, the effective $|\Delta S| \neq 1$, $\Delta Q = 0$ hadronic operator has $|\Delta \vec{P}| = 1$. Since the photon and leptons as well as

$$K_L \sim \bar{\mathfrak{N}}\lambda + \bar{\lambda}\mathfrak{N}$$

are P-spin scalars, the transitions (1.4) and (1.5) are forbidden in the limit of P-spin invariance.

We know that P spin is badly broken in nature. Charmed particles—if they exist—must be much heavier than the observed hadronic states. The question to which we address ourselves here is: How may $K_L \to \mu\mu$ remain strongly suppressed in the broken symmetry case while the suppression of $K_L \to \gamma\gamma$ essentially disappears?

A hint to the solution may be seen by considering low-energy phenomenology.[8] Consider the pole diagram of Fig. 4(a). Both the transitions $K_L \to \pi^0$ and $\pi^0 \to \gamma\gamma$ are allowed by P spin. Similar nonvanishing contributions occur via η and X^0 exchange. As SU(4) is now the basic symmetry, we must add a fourth pseudoscalar meson: $X^{0\prime} \sim \bar{\mathcal{P}}'\mathcal{P}'$. While in the SU(4) limit the contribution of the $X^{0\prime}$ necessarily cancels the others, in the physical world it can be considered negligible:

$$(m_K^2 - m_{X^{0\prime}}^2)^{-1} \ll [m_K^2 - (m_{X^{0,\pi,\eta}})^2]^{-1} .$$

Then we obtain a contribution to $K_L \to \gamma\gamma$ which is of the correct order:

$$\mathcal{A}(K_L \to \gamma\gamma) \sim \mathcal{A}(K_L \to \pi^0)\,\mathcal{A}(\pi^0 \to \gamma\gamma) \sim G_F\alpha .$$

The analogous contribution to $K_L \to \mu\mu$ is shown in Fig. 4(b), where the $\pi^0 \to \mu\mu$ transition can occur via two-photon exchange:

$$\mathcal{A}(K_L \to \mu\mu) \sim \mathcal{A}(K^0 \to \pi^0)\,\mathcal{A}(\pi^0 \to \mu\mu) \sim G_F\alpha^2 ,$$

or via the exchange of a heavy neutral boson (Z) which couples only to $\Delta S = 0$ currents:

$$\mathcal{A}(K_L \to \mu\mu) \sim \mathcal{A}(K^0 \to \pi^0)\,\mathcal{A}(\pi^0 \to \mu\mu) \sim G_F{}^2 m_K{}^2 .$$

Loosely speaking then, one could argue that P spin is an asymptotic symmetry; its validity sets in at energies where hadronic masses are negligible and it serves to eliminate the unwanted high-mass W exchange. At low energies, where weak interactions are truly weak, P spin is so badly broken that it can be disregarded.

A more rigorous argument emerges upon closer examination of the Feynman diagrams for the processes (1.4) and (1.5). The effect of the GIM mechanism is to provide a subtraction for the $\mathcal{P}$-quark propagator:

$$\frac{1}{\not{p}_i - m_{\mathcal{P}}} \to \left(\frac{1}{\not{p}_i - m_{\mathcal{P}}} - \frac{1}{\not{p}_i - m_{\mathcal{P}'}}\right) . \quad (1.10)$$

Since the Feynman integral was convergent before the subtraction, the modified integral remains convergent if we approximate one W propagator by its zero-energy value:

$$(m_W^2 - q^2)^{-1} \simeq m_W{}^{-2} . \quad (1.11)$$

With this approximation the Feynman integral will be correct to order

$$(m_h/m_W)^2 \ll 1 ,$$

where m_h is a hadronic mass. If a process is truly fourth-order semiweak in the sense that two heavy bosons are exchanged, the integral will contain at least one more boson propagator giving an additional factor $m_W{}^{-2}$, so that the resultant amplitude will be of order

$$\frac{g^4}{m_W{}^4} m_h{}^2 \sim G_F{}^2 m_h{}^2 . \quad (1.12)$$

However, if the process is second-order weak and second-order electromagnetic, there will in general be a graph [cf. Figs. 1(b) and 3(b)] in which only one heavy boson is exchanged. Once the approximation (1.11) is made, the remaining integral is independent of the boson mass; then the amplitude must be proportional to

$$g^2/m_W{}^2 e^2 \sim \alpha G_F . \quad (1.13)$$

(In the 't Hooft–Feynman gauge,[9] the contributions of unphysical Higgs scalars are negligible compared to those of the vector bosons.)

As will be seen more explicitly in the following sections, the requirements that the amplitudes for (1.4) and (1.5) be of the correct order are respectively

$$\frac{m_{\varphi'^2} - m_{\varphi}^2}{m_W^2} \ll 1$$

and

$$\frac{m_{\varphi'^2} - m_{\varphi}^2}{m_{\varphi'^2}} \sim 1 \text{ or } m_{\varphi'^2} \gg m_{\varphi}^2 .$$

In other words, P-spin symmetry breaking must be small on the boson mass scale but very large on a hadronic mass scale.

The main body of this paper will be devoted to quantitative calculations within the Weinberg-Salam model of the processes $K \to \mu\bar{\mu}$, $K \to \pi\nu\bar{\nu}$, $K \to \gamma\gamma$, $K \to \pi\gamma\gamma$, and $K \to \pi e\bar{e}$. For this purpose we first estimate the matrix elements for the elementary processes $\lambda \to \mathfrak{N} + l + \bar{l}$ and $\lambda \to \mathfrak{N} + \gamma + \gamma$, and construct phenomenological interactions for free quarks. The matrix elements of such interactions between physical hadronic states can then be estimated, since the hadronic operators which appear are the familiar V-A currents. The neglect of strong-interaction effects may perhaps be justified in models in which quarks are confined in a finite region of space by any of the mechanisms that have recently been suggested (e.g., infrared catastrophe due to non-Abelian gauge fields which prevents the disassociation of "color"-neutral states into "colored" states,[10] or the "bag" mechanism[11]), and within this confinement, quarks are "almost free."

Furthermore, in those theories in which the gauge group of strong interactions commutes with the gauge group of weak and electromagnetic interactions, the $\lambda\mathfrak{N}$-gluon coupling gets transformed away by the wave-function renormalization of quark fields.[12] [Off-shell corrections are expected to be of order $G_F m_h^2 (m_{\varphi'^2} - m_{\varphi}^2)/m_W^2$ and are not important.] Thus, effective two-body operators ($\lambda + \bar{q} \to \mathfrak{N} + \bar{q} + \bar{l}\, l$ or $\gamma\gamma$), which could contribute to $K \to \pi + l\, l$ or $\gamma\gamma$, cannot be induced by gluon exchange in such theories. The contribution of two-body operators which are present in the free-quark model (via $W^{\pm}$ exchange) will be discussed in the appropriate sections. A related, but differently motivated, estimate of higher-order weak interactions has been discussed by Appelquist, Bjorken, and Chanowitz.[13]

In Sec. II, we evaluate the amplitude for $K_L \to \mu\bar{\mu}$ to lowest order in G_F. In the Weinberg-Salam model, this amplitude is found to vanish by what appears to be a fortuitous cancellation between two kinds of diagrams. The general matrix element for the elementary process $\lambda + \bar{\mathfrak{N}} \to l + \bar{l}$ is proportional to the quark mass difference

$$\Delta m^2 = m_{\varphi'^2} - m_{\varphi}^2 .$$

This quantity is estimated by comparing the matrix element of the K_0-$\bar{K}_0$ transition in this approximation with the K_L-K_S mass difference, as the former is proportional to $(\Delta m^2/m_W^2)$. The matrix element so deduced for $\lambda + \bar{\mathfrak{N}} \to l + \bar{l}$ is then applied to estimate the decay rates for $K \to \pi + \nu + \bar{\nu}$. A current-algebra argument is presented here which connects the amplitudes for $K \to l\,\bar{l}$ and $K \to \pi l\,\bar{l}$. Present experimental limits are at a level of 10^{-4}–10^{-5} with respect to $K \to \pi l \nu$ decay rates.

In Sec. III we present the analogous calculation for $K_L \to \gamma\gamma$. A phenomenological discussion of this amplitude is also given in terms of pole contributions [Fig. 4(a)]. The role of P spin is explicitly displayed and it is shown that a reasonable estimate is obtained in the limit of very high φ' mass. The matrix elements for the elementary processes $\lambda + \bar{\mathfrak{N}} \to \gamma + \gamma$ and $\lambda + \bar{\mathfrak{N}} \to \gamma$ are used to estimate the rates for $K \to \pi\gamma\gamma$ and $K \to \pi e\bar{e}$. We comment on the amplitude for $K_S \to \gamma\gamma$, which has the interesting property that the leading contribution vanishes in the free-quark model; we conclude that this decay will be dominated by the absorptive amplitude. The amplitudes for $K^+ \to \pi^+ e\bar{e}$ and $K_S \to \pi^0 e\bar{e}$ are found to be comparatively large, being truly of order $G_F\alpha$. The presently available limit on $K^+ \to \pi^+ e\bar{e}$ is rather stringent; an improvement of the experimental precision by an order of magnitude will severely test our approach.

Section IV contains a summary of our results and comparison with experiment. We also discuss the predictions of other models on the rare decay modes of K mesons.

Finally, the renormalization procedure and details of computations are outlined in appendixes.

In this paper, we shall assume that the mass of the physical Higgs scalar particle is sufficiently large so that its contribution to induced $\Delta S = 1$ transitions is negligible.

Note: In this paper we ignore completely the effects of CP violation. In theories of superweak CP violation, none of the estimates of this paper are affected thereby; in a recent paper, Ma[14] discusses some of the material contained in the present paper.

II. SEMILEPTONIC DECAYS

A. $K \to \mu\bar{\mu}$ and K_L-K_S mass difference

As a prelude to considering the decays $K \to \mu\bar{\mu}$, we shall first discuss the elementary process

$\lambda + \bar{\mathfrak{N}} \to \mu + \bar{\mu}$, in the free-quark model. There are two classes of diagrams contributing to this process. One is the diagram in which a pair of W^+ and W^- is exchanged between the quark and lepton lines. The second class of diagrams is generated by the "induced" $\lambda\mathfrak{N}Z$ coupling (Fig. 5). The evaluation of these diagrams, to the lowest order in m_W^{-2}, is outlined in Appendixes B and C.

When the GIM mechanism is incorporated into the Weinberg-Salam model, the W^+W^- contribution to the process $\lambda + \bar{\mathfrak{N}} \to l + \bar{l}$ is, in the 't Hooft–Feynman gauge,

$$-i\frac{G_F}{\sqrt{2}}\frac{\alpha}{\pi}\cos\theta_C \sin\theta_C\, \epsilon\bar{\mathfrak{N}}\gamma^\alpha\left[\tfrac{1}{2}(1-\gamma_5)\right] \times\lambda\left\{\tfrac{1}{2}\bar{\mu}\gamma_\alpha\left[\tfrac{1}{2}(1-\gamma_5)\right]\mu - 2\bar{\nu}\gamma_\alpha\left[\tfrac{1}{2}(1-\gamma_5)\right]\nu\right\}, \tag{2.1}$$

$$\epsilon = (\Delta m^2/m_W^2 \sin^2\theta_W)\left[\ln(m_W^2/m_{\mathcal{P}'}^2) - 1\right]$$

and similarly for the electronic leptons, where $m_W^2 \sin^2\theta_W \simeq (38\ \mathrm{GeV})^2$, θ_C is the Cabibbo angle, and $\Delta m^2 \equiv m_{\mathcal{P}'}^2 - m_{\mathcal{P}}^2$ is the difference of masses squared of the $\mathcal{P}$ and $\mathcal{P}'$ quarks. In the presence of the GIM mechanism, there is no $\lambda\mathfrak{N}Z$ coupling, but such a coupling is induced in higher orders. The effective $\lambda\mathfrak{N}Z$ coupling, to lowest order in α, and in m_W^{-2}, is given in (A1); the contribution of the Z exchange to the process is

$$-i\frac{G_F}{\sqrt{2}}\frac{\alpha}{\pi}\cos\theta_C \sin\theta_C\, \epsilon\bar{\mathfrak{N}}\gamma^\alpha\left[\tfrac{1}{2}(1-\gamma_5)\right]\lambda \times\left(\mu\gamma_\alpha\left\{-\tfrac{1}{2}\left[\tfrac{1}{2}(1-\gamma_5)\right] - \sin^2\theta_W\right\}\mu + \tfrac{1}{2}\bar{\nu}\gamma_\alpha\left[\tfrac{1}{2}(1-\gamma_5)\right]\nu\right). \tag{2.2}$$

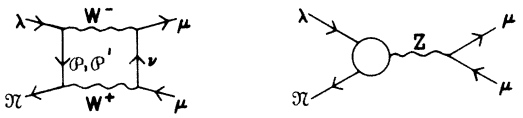

FIG. 5. Two classes of diagrams for $\lambda + \bar{\mathfrak{N}} \to \mu + \bar{\mu}$. The definition and evaluation of the effective $\lambda\mathfrak{N}Z$ vertex (represented by a circle in the lower diagram) are given in Appendix B.

The total amplitude for $\lambda + \mathfrak{N} \to l + \bar{l}$ is given therefore by

$$iT(\lambda + \mathfrak{N} \to l + l) \simeq \frac{G_F}{\sqrt{2}}\frac{\alpha}{\pi}\,\epsilon\cos\theta_C \sin\theta_C\left\{\bar{\mathfrak{N}}\gamma_\alpha\left[\tfrac{1}{2}(1-\gamma_5)\right]\lambda\right\}\left\{\bar{\mu}\gamma_\alpha\mu \sin^2\theta_W + \tfrac{1}{2}\bar{\nu}\gamma_\alpha\left[\tfrac{1}{2}(1-\gamma_5)\right]\nu\right\}, \tag{2.3}$$

where

$$\epsilon \simeq \frac{\Delta m^2}{(38\ \mathrm{GeV})^2}\ln\frac{m_W^2}{m_{\mathcal{P}'}^2} \tag{2.4}$$

is the suppression factor arising from the GIM mechanism.

In order to estimate the decay rate $K_{L,S} \to \mu\bar{\mu}$ we take the matrix element of (2.3) between the $K_{L,S}$ state and the vacuum, and use the partially conserved axial-vector current (PCAC) principle. In this way we obtain

$$T(K_S \to \mu\bar{\mu}) = 0, \tag{2.5}$$

$$T(K_L \to \mu\bar{\mu}) = -\sqrt{2}\,\frac{G_F}{\sqrt{2}}\frac{\alpha}{2\pi}\,\epsilon\cos\theta_C \sin\theta_C\left[if_K(p_K)^\alpha\right] \times\sin^2\theta_W\,\bar{\mu}\gamma_\alpha\mu = 0,$$

where $f_K \sin\theta_C \simeq 33$ MeV. The $T(K_L \to \mu\bar{\mu})$ amplitude vanishes because $(p_K)^\alpha\,\bar{\mu}\gamma_\alpha\mu = 0$. The vanishing of this amplitude is due to the fortuitous cancellation of the axial-vector part $\bar{\mu}\gamma_\alpha\gamma_5\mu$ between the W^+W^- and Z contributions, (2.1) and (2.2). Even when the effects of strong interactions are taken into account, it is probable that these two contributions cancel to a large extent (especially if strong interactions are described by an asymptotically free field theory). We suggest that the dominant mechanism for $K_{L,S} \to \mu\bar{\mu}$ are the conventional ones[15]: $K_L \to \gamma\gamma \to \mu\bar{\mu}$, $K_S \to \pi\pi \to \gamma\gamma \to \mu\bar{\mu}$. Then we expect

$$\frac{\Gamma(K_S \to \mu\bar{\mu})}{\Gamma(K_L \to \mu\bar{\mu})} \simeq \frac{\Gamma(K_S \to \gamma\gamma)}{\Gamma(K_L \to \gamma\gamma)}. \tag{2.6}$$

As we shall see in Sec. III, we expect $\Gamma(K_S \to \gamma\gamma) \approx 2\Gamma(K_L \to \gamma\gamma)$.

To estimate the size of ϵ we consider the $K_L K_S$ mass difference. In Appendix F, we evaluate the effective Lagrangian for $\lambda + \bar{\mathfrak{N}} \to \bar{\lambda} + \mathfrak{N}$ in our approximation and obtain

$$\mathcal{L}_{\mathrm{eff}} = -\frac{G_F}{\sqrt{2}}\frac{\alpha}{4\pi}\,\epsilon_0\cos^2\theta_C \sin^2\theta_C\left[\bar{\lambda}\gamma_\alpha\left[\tfrac{1}{2}(1-\gamma_5)\right]\mathfrak{N}\right]^2 + \mathrm{H.c.}, \tag{2.7}$$

where ϵ_0 is defined in Appendix F, (F4)–(F5). In order to estimate the magnitude of the $K^0\bar{K}^0$ transition amplitude, we insert the vacuum state between two currents in all possible ways and use PCAC (it is admittedly a dubious procedure, but it will not mislead us as to the order of magnitude):

$$\langle\bar{K}^0|-\mathcal{L}_{\mathrm{eff}}|K^0\rangle \simeq \frac{G_F}{\sqrt{12}}\frac{\alpha}{4\pi}\,\epsilon_0\cos^2\theta_C \sin^2\theta_C\, 4(\tfrac{1}{2})^2 \times\langle\bar{K}^0|\bar{\mathfrak{N}}\gamma^\alpha\gamma_5\lambda|0\rangle\langle 0|\bar{\mathfrak{N}}\gamma_\alpha\gamma_5\lambda|K^0\rangle = \frac{G_F}{\sqrt{2}}f_K^2 m_K^2\frac{\alpha}{4\pi}\,\epsilon_0\cos^2\theta_C \sin^2\theta_C.$$

(This estimate is for a triplet-quark scheme; for the 3-color quarks, the above equation should be multiplied by $\frac{2}{3}$.)

The K_L-K_S mass difference is given by

$$m_L - m_S = m_K(1+m_K^{-2}\langle\bar{K}^0|-\mathcal{L}_{\rm eff}|K^0\rangle)^{1/2} - m_K(1-m_K^{-2}\langle\bar{K}^0|-\mathcal{L}_{\rm eff}|K^0\rangle)^{1/2} \simeq \frac{1}{m_K}\langle\bar{K}^0|-\mathcal{L}_{\rm eff}|K^0\rangle .$$

Thus,

$$\frac{m_L-m_S}{m_K} \simeq \frac{G_F}{\sqrt{2}} f_K^2 \frac{\alpha}{4\pi}\epsilon_0 \sin^2\theta_C\cos^2\theta_C \simeq \epsilon_0\times 5\times 10^{-12} . \tag{2.8}$$

Experimentally the left-hand side is about 0.7×10^{-14}, so we have

$$\epsilon_0 \simeq 1.4\times10^{-3} .$$

Equation (2.8) is compatible [see Eqs. (F4)–(F5)] either with $m_{\mathcal{P}'}\simeq m_{\mathcal{P}}$ and large, and $m_{\mathcal{P}'}-m_{\mathcal{P}}\simeq 1$ GeV, or $m_{\mathcal{P}}\ll m_{\mathcal{P}'}$ and $m_{\mathcal{P}'}\simeq 1.5$ GeV. We argue in Sec. III, in connection with the nonsuppression of the $K_L\to\gamma\gamma$ rate, that the latter is the logically tenable alternative. In this case

$$\epsilon \simeq \epsilon_0|\ln(\epsilon_0\sin^2\theta_W)| \simeq 10^{-2} . \tag{2.9}$$

What is the meaning of the suppression factor ϵ? The expression (2.4), couched as it is in the language of the free-quark model, is hard to interpret in the context of a realistic model. Nevertheless, it indicates the degree to which the GIM cancellation mechanism must be effective, and suggests that charmed meson states cannot be too massive. We suggest that in a more realistic model (which we shall discuss elsewhere) the suppression factor will take the form

$$\epsilon \sim \frac{m_c^2}{m_W^2\sin^2\theta_W}\ln\frac{m_W^2}{m_c^2}$$

in the limit of chiral SU(3)×SU(3) symmetry, where m_c is the average mass of the charmed pseudoscalar mesons. If this is correct, we expect m_c to be less than, say, a few GeV. The experimental implications of the existence of charmed mesons have already been discussed by GIM, Snow, and others.[15]

Finally, with the suppression factor ϵ of the order (2.9), the weak contribution to $K_L\to\mu\mu$ would be well within the bounds implied by the experimental data even if the cancellation of the axial-vector part were not complete.

B. $K\to\pi\nu\bar{\nu}$

The effective interaction derived in (A7) for the elementary process $\lambda+\bar{\mathfrak{N}}\to l+\bar{l}$ allows us to estimate the rates for $K^+\to\pi+\nu+\bar{\nu}$. Noting that

$$\langle\pi^+|\bar{\mathfrak{N}}\gamma_\mu(1-\gamma_5)\lambda|K^+\rangle = [(p_+)_\mu f_+ + (p_-)_\mu f_-] = \sqrt{2}\,\langle\pi^0|\bar{\mathfrak{N}}\gamma_\mu(1-\gamma_5)\lambda|K^0\rangle = -\sqrt{2}\langle\pi^0|\bar{\lambda}\gamma_\mu(1-\gamma_5)\mathfrak{N}|\bar{K}^0\rangle,$$

where f_+ and f_- are the K_{l3} form factors, and $p_\pm = p_K \pm p_\pi$, we find that

$$iT(K^+\to\pi^+\nu\bar{\nu}) = i\frac{G_F}{\sqrt{2}}\frac{\alpha}{2\pi}\epsilon\cos\theta_C\sin\theta_C \times[(p_+)_\mu f_+ + (p_-)_\mu f_-] \times[3\bar{\nu}\gamma^\mu[\tfrac{1}{2}(1-\gamma_5)]\nu] = iT(K_1^0\to\pi^0\nu\bar{\nu}) , \tag{2.10}$$

and

$$iT(K_2\to\pi^0\nu\bar{\nu}) = 0 . \tag{2.11}$$

Thus, if we neglect the electron mass

$$\frac{\Gamma(K^+\to\pi^+\nu\bar{\nu})}{2\Gamma(K^+\to\pi^0\bar{e}\nu)} = \frac{\Gamma(K_S\to\pi^0\nu\bar{\nu})}{\Gamma(K_L\to\pi e\nu)} = 2\left(\frac{3\alpha}{4\pi}\epsilon\cos\theta_C\right)^2 , \tag{2.12}$$

where

$$\Gamma(K_L\to\pi e\nu) = \Gamma(K_L\to\pi^-\bar{e}\nu)+\Gamma(K_L\to\pi^+e\bar{\nu})$$

and the factor 2 on the right-hand side of (2.12) comes from summing over two kinds of neutrinos. Together with the limit on ϵ given in (2.6), we obtain

$$2\left(\frac{3\alpha}{4\pi}\epsilon\cos\theta_C\right)^2 \simeq 10^{-9}$$

and

$$\frac{\Gamma(K^+\to\pi^+\nu\bar{\nu})}{\Gamma(K^+\to\text{all})} \simeq 10^{-10} , \tag{2.13}$$

$$\frac{\Gamma(K_S\to\pi^0\bar{\nu}\nu)}{\Gamma(K_S\to\text{all})} \simeq 10^{-12} , \tag{2.14}$$

$$\frac{\Gamma(K_L\to\pi^0\bar{\nu}\nu)}{\Gamma(K_S\to\pi^0\bar{\nu}\nu)} \simeq 10^{-4} . \tag{2.15}$$

The last follows from the fact that, as implied in (2.11), the amplitude for $K_L\to\pi^0\bar{\nu}\nu$ is at most of order $G_F\alpha\epsilon^2$.

The results of (2.10) and (2.11) based on the simple quark model, obtained by neglecting all but the one-body operator deduced by looking at the process $\lambda+\bar{\mathfrak{N}}\to l+\bar{l}$, may appear more suspect than those of Sec. II A. However, in this theory, there is a soft-pion theorem relating the $K\to\pi l\bar{l}$ and $K^0\to l\bar{l}$ amplitudes, and our results are consistent with it.

In the case $m_{\mathcal{P}}$, $m_{\mathfrak{N}}\ll m_{\mathcal{P}'}$, the chiral SU(2)

$\times$SU(2) is a good symmetry, and the entire Lagrangian commutes with the generators $Q^i + Q_5^i$ of the right-handed chiral SU(2) group approximately (noncommuting pieces being of order m_φ/m_W), except for the couplings of the Z meson and the photon to quarks. Thus, except for the Z-meson reducible diagrams, we have the soft-pion theorem

$$\lim_{q\to 0} T^{\rm irr}(K_{S,L}(p) \to \pi^0(q)\,\nu(r)\,\bar\nu(p-q-r)) = i\frac{1}{\sqrt{2}f_\pi}\,T^{\rm irr}(K_{L,S}(p)\to\nu(r)\,\bar\nu(p-r))\ , \quad (2.16)$$

$$\lim_{q\to 0} T^{\rm irr}(K^+(p) \to \pi^+(q)\,\nu(r)\,\bar\nu(p-q-r)) = i\frac{1}{f_\pi}\,T^{\rm irr}(K^0(p)\to\nu(r)\,\bar\nu(p-r))\ , \quad (2.17)$$

where ν and $\bar\nu$ are not in general on their mass shells and $T^{\rm irr}$ denotes the single-particle irreducible amplitude. Equation (2.16) follows from the standard current-algebra manipulation.[17]

Let us now consider the Z-meson reducible diagrams. The effective πKZ vertex is of the form

$$\left\langle \pi(q)\left| T\left\{ j_\mu^Z(0)\exp\left[(+i)\int d^4y\,\mathfrak{L}_W(y)\right]\right\}\right| K(p)\right\rangle$$

where $\mathfrak{L}_W$ is the weak-interaction Lagrangian ($\mathfrak{L}_W$ includes the couplings of gauge bosons and Higgs scalars to fermions, and the interactions of weak boson fields; since we are interested in the matrix element to lowest nonvanishing order, we may ignore the couplings of the Z meson and the photon to fermions, as well as any complications that might arise from the presence of the Feynman–DeWitt–Popov–Faddeev ghost fields). The part of j_μ^Z which does not commute with the right-handed chiral charge $Q^\pm + Q_5^\pm$ is $-\sin^2\theta_W j_\mu^\gamma$, where j_μ^γ is the electromagnetic current. Because j_μ^γ is conserved, the effective $K\pi\gamma$ vertex must have the form

$$\left\langle \pi^+(q)\left| T\left\{ j_\mu^\gamma(0)\exp\left[i\int d^4y\,\mathfrak{L}_W(y)\right]\right\}\right| K^+(p)\right\rangle = (k^2 g_{\mu\nu} - k_\mu k_\nu)(p+q)^\nu\,G(t)\ , \quad (2.18)$$

where

$$k = p - q, \quad t = k^2\ .$$

The proof follows from the usual Ward identity, and is essentially identical to the one we present in Appendix D for the effective $\lambda\mathfrak{N}\gamma$ vertex. On dimensional grounds, we have

$$G(0) = O(G_F e)\ . \quad (2.19)$$

On the other hand, the matrix element of the purely left-handed current $j_\mu^Z - (-\sin^2\theta_W j_\mu^\gamma)$, *which is not conserved,* is of the form

$$\left\langle \pi(q)\left| T\left\{ [j_\mu^Z(0) + \sin^2\theta_W j_\mu^\gamma(0)]\exp\left[i\int d^4y\,\mathfrak{L}_W(y)\right]\right\}\right| K(p)\right\rangle = (p+q)_\mu F_+(t) + (p-q)_\mu F_-(t)\ , \quad (2.20)$$

where

$$F_+(0),\ F_-(0) = O(G_F e m_c^2)\ . \quad (2.21)$$

Thus, Eqs. (2.16) and (2.17) should hold also for the full amplitudes, to lowest order in $(t/m_c^2) \sim (m^2/m_c^2)$ [i.e., neglecting contributions of order (m^2/m_W^2) compared to (m_c^2/m_W^2)], where m is the typical uncharmed hadron mass.

The chiral charge $Q^3 + Q_5^3$ does commute with the electromagnetic current, so that the soft-pion theorem (2.16) holds actually for the full amplitude. Let us parametrize the $K_{L,S} \to \pi^0\nu\bar\nu$ amplitude by

$$T(K(p)\to\pi^0(q)\,\nu(r)\,\bar\nu(p-q-r)) = [A(p+q)^\mu + B(p-q)^\mu + Cr^\mu + iD\epsilon^{\mu\nu\rho\sigma}p_\nu q_\rho r_\sigma]\times\bar\nu\gamma_\mu(1-\gamma_5)\nu\ , \quad (2.22)$$

where A, B, C, and D are, in general, invariant functions of the momenta p, q, and r. In the soft-pion limit we have

$$A_L + B_L = 0\ ,$$
$$A_S + B_S = \left(\frac{f_K}{f_\pi}\right)\frac{G_F}{\sqrt{2}}\,\frac{3\alpha}{4\pi}\,\epsilon\cos\theta_C\sin\theta_C\ , \quad (2.23)$$
$$C_{L,S} = 0\ ,$$

where we have used the amplitudes for $K_{L,S} \to \nu\bar\nu$ (off shell) deduced from (2.3). The amplitude (2.10) is consistent with (2.22), (2.23) when the Callan-Treiman relation[18] is taken into account. Note further that if we neglect the momentum dependence of the form factors, CP invariance alone implies

$$A_L = B_L = C_L = 0\ ,$$
$$D_S = 0\ . \quad (2.24)$$

These constraints follow from CP invariance and the assumptions that the neutrino is left-handed and massless. In most models the form factor D is identically zero and $K_L \to \pi\bar\nu\nu$ is strongly suppressed.

III. ELECTROMAGNETIC DECAYS

A. $K \to \gamma\gamma$: Quark model

We shall first discuss the free-quark-model calculations in analogy to our discussion of the leptonic decays. However, as the estimates we obtain appear *a posteriori* less reliable, we shall show in the case of $K_L \to \gamma\gamma$ that a similar estimate can be obtained from low energy phenomenology. In both cases the numbers we use should be taken as order of magnitude estimates.

The first step in the calculation is to obtain an effective Lagrangian for the process $\lambda + \bar{\mathfrak{N}} \to \gamma + \gamma$. There are two classes of diagrams here. The first consists of those diagrams which are one-quark reducible (see Fig. 6). The $\lambda \mathfrak{N} \gamma$ vertex is discussed in Appendix D (see also Appendix B). For the real-photon emission the transition charge form factor vanishes; the nonvanishing effects of these diagrams come from the $\lambda \to \mathfrak{N}$ transition magnetic moment as well as the off-shell correction due to the internal quark lines. These effects are, however, of order $\epsilon \sim (\Delta m_{\mathcal{P}'}{}^2/m_W{}^2)\ln(m_W{}^2/m_{\mathcal{P}'}{}^2)$ compared to the main term we shall consider, and shall be ignored.

The second class of diagrams consists of one-particle irreducible ones. As is shown explicitly in Appendix E, the leading contribution comes from the Feynman diagrams in which only one heavy boson is exchanged (Fig. 7). From the point of view of spin dependence, the graphs of Fig. 7(a) are identical to those of Fig. 7(b), which are obtained from the former by means of a Fierz-Michel transformation,

$$[\bar{\mathfrak{N}}\gamma_\mu(1-\gamma_5)\mathcal{P}][\bar{\mathcal{P}}\gamma^\mu(1-\gamma_5)\lambda] = [\bar{\mathfrak{N}}\gamma_\mu(1-\gamma_5)\lambda] \times [\bar{\mathcal{P}}\gamma^\mu(1-\gamma_5)\mathcal{P}] ,$$

where the anticommutativity of the quark fields is taken into account. Note that this transformation is possible only because the heavy boson propagator is $-g_{\mu\nu}(p^2 - m_W{}^2)^{-1}$ in the 't Hooft–Feynman gauge (see Appendix A). Then the effective interaction takes the form of a current operator

$$J_\mu^0 = \bar{\mathfrak{N}}\gamma_\mu(1-\gamma_5)\lambda \tag{3.1}$$

multiplying a closed-loop integral, where the integrand includes the W propagator. Apart from the W propagator, the integral involved is identical to that studied by Rosenberg and Adler.[19] Recall that the latter is linearly divergent, and therefore its value depends on the choice of integration variables and on the way in which the integration is performed; this ambiguity is removed by requiring that the result be gauge-invariant with respect to both photons.

In our case the boson propagator makes the integral convergent and its value is unambiguous. However, if only, say, the $\mathcal{P}$-quark loop is considered the result is not gauge-invariant. Other graphs must contribute gauge noninvariant terms of order $m_W{}^{-2}$ which render the total amplitude gauge-invariant to that order. However, the gauge-noninvariant piece of the graphs in Fig. 7(a) is independent of the quark mass, and cancels out when the $\mathcal{P}$- and $\mathcal{P}'$-quark diagrams are summed. Thus for our purposes it is sufficient to consider only the one-W-exchange diagrams, as anticipated in the Introduction. See Appendix E for estimates of order of magnitude of various diagrams; the integral is evaluated in Appendix A. To order $m_W{}^{-2}$, the effective operator for the transition is given by

$$i(J_\mu^0 + J_\mu^{0\dagger})\, T^\mu_{\rho\sigma} , \tag{3.2}$$

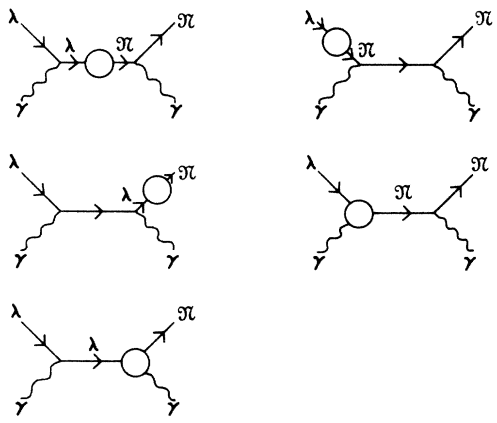

FIG. 6. One-quark reducible diagrams for $\lambda + \bar{\mathfrak{N}} \to \gamma + \gamma$.

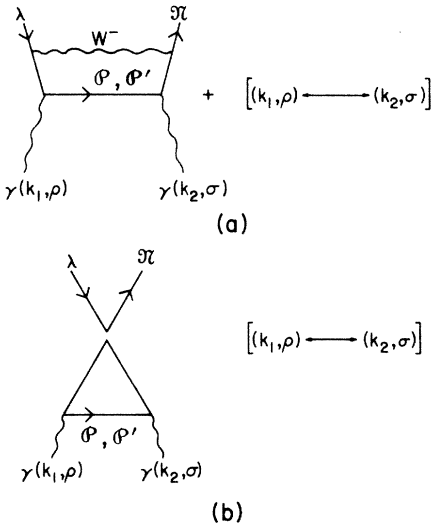

FIG. 7. Leading contributions to $\lambda + \bar{\mathfrak{N}} \to \gamma + \gamma$. To leading order in $M_W{}^{-2}$, the diagrams in (a) reduce to those of (b).

where the amplitude $T^{\mu}_{\rho\sigma}$ may be read off (A14).

To obtain the amplitude for $K_L \to \gamma\gamma$ we must take the matrix element of the current operator (3.1) between K_L and the vacuum:

$$\langle 0|J^0_\mu|K_L\rangle = \langle 0|J^{0\dagger}_\mu|K_L\rangle = i\frac{1}{\sqrt{2}} f_K (p_K)_\mu \ . \tag{3.3}$$

Contracting $(p_K)_\mu = (k_1 + k_2)_\mu$ with $T^{\mu}_{\rho\sigma}$ we obtain

$$iT(K_L \to \gamma\gamma) = iF_{\mu\nu}(k_1)\tilde{F}^{\mu\nu}(k_2)\frac{G_F}{\sqrt{2}}\frac{2\alpha}{\pi}\cos\theta_C \sin\theta_C \times (i\sqrt{2} f_K) A_\gamma \ , \tag{3.4}$$

where

$$A_\gamma = Q^2\left[F\left(\frac{m_{\mathcal{P}}^2}{m_K^2}\right) - F\left(\frac{m_{\mathcal{P}'}^2}{m_K^2}\right)\right] \ , \tag{3.5}$$

Q being the charge of the $\mathcal{P}$ quark. The function $F(\beta)$ is defined in (A12) and plotted in Fig. 8. For $\beta > 1$, $F(\beta)$ converges rapidly to zero. If we assume that both quark masses $m_{\mathcal{P}}$ and $m_{\mathcal{P}'}$ are very heavy compared to the kaon mass, we obtain a strong suppression of $K_L \to \gamma\gamma$ in contradiction with experiment. However, in the range $0 \leq \beta \leq 1$, $F(\beta)$ is a rapidly varying function with values in the range

$$-\tfrac{1}{2} \lesssim F(\beta) \lesssim \tfrac{1}{2}, \quad \text{for } 0 \leq \beta \leq 1 \ .$$

If A_γ is treated as a phenomenological parameter as defined by Eq. (3.4), then using the experimental branching ratio

$$\frac{\Gamma(K_L \to \gamma\gamma)}{\Gamma(K_L \to \text{all})} = (4.9 \pm 0.4) \times 10^{-4} \tag{3.6}$$

we obtain the empirical determination

$$|A_\gamma| = 0.87 \pm 0.04 \ . \tag{3.7}$$

Assuming $m_{\mathcal{P}'} \gg m_K \gtrsim m_{\mathcal{P}}$, the free-quark model seems to be compatible with the nonsuppression of the process $K_L \to \gamma\gamma$. (Another solution, which in fact fits the data better for $Q^2 = \frac{4}{9}$, is $m_{\mathcal{P}'} \approx m_K/2$, $m_{\mathcal{P}} \lesssim m_K/4$. Such a low mass for $m_{\mathcal{P}}$ is not really ruled out by the K_L-K_S mass difference because of the approximation made in evaluating (2.7). However, this interpretation perhaps takes too literally the low mass region of Fig. 8.) Note incidentally that the expression (3.5) is valid in the color-quark scheme as well as in the one-triplet model.

To lowest order in m_W^{-2}, there is no term which leads to the CP even state of 2γ. This is most easily seen in Fig. 7 by noting that the VVV vertex in question vanishes by Furry's theorem. However, phenomenologically, $K_S \to \gamma\gamma$ can proceed through the 2π intermediate state; we shall interpret the quark-model result to mean that the real part of the $K_S \to \gamma\gamma$ amplitude is of order ϵ compared to the $K_L \to \gamma\gamma$ amplitude and negligible. [Note further that $K_S \to \gamma\gamma$ is forbidden by U spin in the exact SU_3 limit.] The 2π contribution to the absorptive part of the $K_S \to \gamma\gamma$ amplitude has been estimated. It is[20]

$$\Gamma(K_S \to \gamma\gamma) \simeq 2 \times 10^4 \text{ sec}.$$

Thus we have

$$\Gamma(K_S \to \gamma\gamma)/\Gamma(K_L \to \gamma\gamma) \simeq 2. \tag{3.8}$$

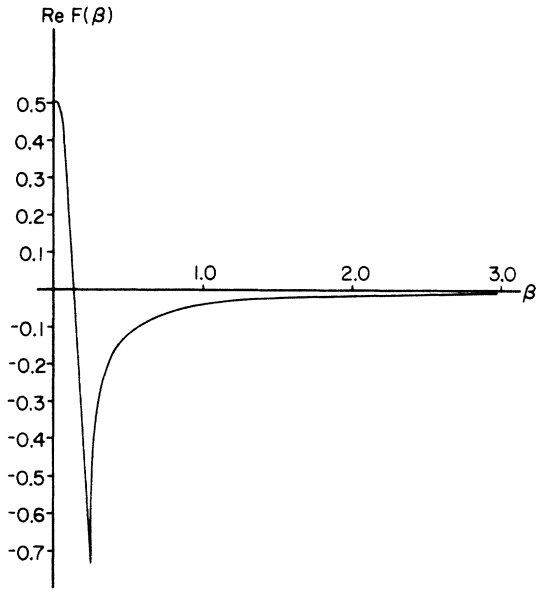

FIG. 8. Re$F(\beta)$ vs β. $F(\beta)$ is defined in (A12). The figure is the result of a numerical integration of (A12). Courtesy of Professor Chris Quigg.

B. $K_L \to \gamma\gamma$: Phenomenological analysis

In this section we shall estimate the amplitude for $K_L \to \gamma\gamma$ using the pole diagrams of Fig. 4(a). We define the following set of meson states in terms of their quark content:

$$\pi^0 = (\bar{\mathcal{P}}\mathcal{P} - \bar{\mathfrak{N}}\mathfrak{N})/\sqrt{2} \ ,$$

$$\eta_8 = (\bar{\mathcal{P}}\mathcal{P} + \bar{\mathfrak{N}}\mathfrak{N} - 2\bar{\lambda}\lambda)/\sqrt{6} \ ,$$

$$\eta_0 = (\bar{\mathcal{P}}\mathcal{P} + \bar{\mathfrak{N}}\mathfrak{N} + \bar{\lambda}\lambda)/\sqrt{3} \ ,$$

$$\eta_c = \bar{\mathcal{P}}'\mathcal{P}' \ .$$

The isoscalar states can, of course, mix; we label the physical states by η, X^0, and X_c.

The effective nonleptonic weak interaction transforms as the first component of a U-spin vector and the third component of a P-spin vector:

$$\mathfrak{L}_{\text{weak}} \sim (\bar{\mathfrak{N}}\lambda + \bar{\lambda}\mathfrak{N})(\bar{\mathcal{P}}\mathcal{P} - \bar{\mathcal{P}}'\mathcal{P}') \ .$$

Neglecting symmetry-breaking corrections, the phenomenological coupling of K_L to the neutral-

meson system must be of the form

$$\mathcal{L}_{\text{weak}} = cK_L\left(\frac{\pi^0}{\sqrt{2}} + \frac{\eta_8}{\sqrt{6}} + \frac{\eta_0}{\sqrt{3}} - \eta_c\right) \equiv K_L \sum_i c_i P_i \,. \tag{3.9}$$

The electromagnetic coupling is a scalar in both U spin and P spin:

$$\mathcal{L}_{\text{em}} \sim F_{\mu\nu}\tilde{F}_{\mu\nu}[A(\bar{\Phi}\Phi + \bar{\Phi}'\Phi') + B(\bar{\Pi}\Pi + \bar{\lambda}\lambda)] \,.$$

If we assume that the amplitude for $P_i \to \gamma\gamma$ is determined by a single quark loop, we may interpret A and B as the squared charges of the quarks:

$$\begin{aligned}\mathcal{L}_{\text{em}} &\equiv d\,\tilde{F}_{\mu\nu}F_{\mu\nu}\left[Q^2\left(\frac{\pi^0}{\sqrt{2}} + \frac{\eta_8}{\sqrt{6}} + \frac{\eta_0}{\sqrt{3}} + \eta_c\right)\right. \\ &\qquad \left. + (Q-1)^2\left(\frac{2\eta_0}{\sqrt{3}} - \frac{\pi^0}{\sqrt{2}} - \frac{\eta}{\sqrt{6}}\right)\right] \\ &\equiv \tilde{F}_{\mu\nu}F_{\mu\nu}\sum_i d_i P_i \,. \end{aligned} \tag{3.10}$$

It is obvious from (3.9) and (3.10) that pole contribution to $K_L \to \gamma\gamma$ is forbidden in the limit of mass degeneracy, since $\sum c_i d_i = 0$. When mass splitting is present the amplitude takes the form

$$\mathcal{A}(K_L \to \gamma\gamma) = c_i (m_K^2 - M^2)^{-1}_{ij} d_j + \frac{c_\pi d_\pi}{m_K^2 - m_\pi^2} \,, \tag{3.11}$$

where M^2 is the 3×3 matrix which describes the isoscalar meson masses and their mixing:

$$\mathcal{L}_{\text{mass}} = P_i M^2_{ij} P_j \,. \tag{3.12}$$

In the Weinberg model SU(4) is broken by the quark mass splitting; to lowest order in the symmetry breaking the meson masses may be described by an effective Lagrangian of the form

$$\begin{aligned}\mathcal{L}_{\text{mass}} &= m_0(\mathrm{Tr}\pi)^2 + m_1 \mathrm{Tr}\pi^2 + \alpha\,\mathrm{Tr}\pi\Delta M\pi \\ &\quad + \beta\,\mathrm{Tr}\pi\,\mathrm{Tr}\Delta M\pi \,, \end{aligned} \tag{3.13}$$

where π is the 4×4 matrix representation of the pseudoscalar states (15-plet plus singlet) and ΔM is a traceless diagonal matrix with two independent elements: $m_\lambda - m_\Phi$, $m_{\Phi'} - m_\Phi$. The matrix elements M^2_{ij} in (3.12) can be extracted from (3.13).

Explicit evaluation of the amplitude (3.11) in the general case is quite involved. If we restrict ourselves to the case of fractionally charged quarks, we obtain

$$\mathcal{A}(K_L \to \gamma\gamma) = h\left(\frac{N}{D} + \frac{1}{2\Delta m^2}\right), \quad h = \tfrac{1}{3}cd \,. \tag{3.14}$$

The last term is just the pion pole

$$\Delta m^2 = m_K^2 - m_\pi^2 \,.$$

The first term is given by the relations

$$\begin{aligned} D &= \mathrm{Det}(m_K^2 - M^2) \\ &= (m_K^2 - m_\eta^2)(m_K^2 - m_{X^0}^2)(m_K^2 - m_{X_c}^2) \end{aligned}$$

and

$$N = -\frac{D}{2\Delta m^2} + 4(\tfrac{1}{3}\Delta m^2)\Delta m_c^2(2 + 8\gamma + 3\gamma^2) \,,$$

where $\gamma = \beta/\alpha$ and

$$\Delta m_c^2/\Delta m^2 = (m_{\Phi'} - m_\Phi)/(m_\lambda - m_\Phi) \,.$$

The pion pole is exactly canceled by the residue at the η pole and we obtain

$$\mathcal{A}(K_L \to \gamma\gamma) = \frac{m_K^2 - m_\pi^2}{3(m_K^2 - m_\eta^2)} \frac{hK}{(m_K^2 - m_{X^0}^2)} \,, \tag{3.15}$$

with

$$K = 4(2 + 8\gamma + 3\gamma^2)\Delta m_c^2/(m_K^2 - m_{X_c})^2 \,.$$

While the result is finite and nonvanishing in the SU(3) limit, it vanishes in the P-spin limit since $\Delta m_c^2 \to 0$ does not require $m_K^2 \to m_{X_c}^2$:

$$D \sim \Delta m^2(a\Delta m^2 + b\Delta m_c^2) \,.$$

For the physical case of badly broken P spin we assume

$$m_{X_c}^2 - m_K^2 \gg m_{X^0}^2 - m_K^2 \,.$$

In this limit the X_0, X_c mixing is proportional to γ; assuming small mixing we find

$$\begin{aligned} m_{X_c}^2 &\simeq 2(1+\gamma)\Delta m_c^2 \,, \\ K &\simeq -2(2 + 8\gamma + 3\gamma^2)/(1+\gamma) \,. \end{aligned} \tag{3.16}$$

The amplitude (3.15) is very sensitive to the value of γ which also determines the X^0, η mixing parameter. The value $\gamma \simeq -0.6$ corresponds to small mixing as experimentally determined.

For comparison of the amplitude (3.15) with experiment we must evaluate the effective coupling constant h. If A_π is defined as the pion-pole contribution to (3.14),

$$A_\pi = \mathcal{A}(K_L \to \pi^0)\mathcal{A}(\pi^0 \to \gamma\gamma)/(m_K^2 - m_\pi^2) \,,$$

we have

$$h = 2\Delta m^2 A_\pi$$

and

$$\begin{aligned} \mathcal{A}(K_L \to \gamma\gamma) &= \tfrac{2}{3}\frac{(m_K^2 - m_\pi^2)}{(m_K^2 - m_\eta^2)} \frac{A_\pi K}{(m_K^2 - m_{X^0}^2)} \,, \\ &\approx A_\pi K \,. \end{aligned} \tag{3.17}$$

The transition amplitude for $K_L \to \pi^0$ can be estimated using current algebra[17]:

$$\mathcal{A}(K_L \to \pi) = -i\sqrt{2}\, f_\pi\, \mathcal{A}(K_S \to \pi^0\pi^0) \,. \tag{3.18}$$

Then using the decay rates for $\pi \to \gamma\gamma$ and $K_S \to \pi^0\pi^0$

we find

$$|A_\pi/A_{\rm obs}| = 2.3 \pm 0.1, \tag{3.19}$$

where $A_{\rm obs}$ is the experimentally determined amplitude for $K \to \gamma\gamma$.

From Eq. (3.16) it is clear that the parameter K is very sensitive to the pseudoscalar mixing. A value of $|K| \simeq 0.5$ would reproduce the experimental amplitude. This is achieved with $\gamma \simeq -0.3$, which, however, gives too strong a mixing for the X^0, η system. We may also argue that a perturbative treatment of SU(4) breaking is meaningless, and simply neglect the contribution of $\eta_c \simeq X_c$. Using the experimentally determined masses and mixing angle for η and X^0 we obtain $K \simeq -1.5$. If we also neglect the η, X^0 mixing, the amplitude (3.15) reduces to the X^0 pole with $K = -\frac{2}{3}$.

Considering the approximations and uncertainties involved, the pole amplitudes can adequately account for the observed decay rate.

C. $K \to \pi\gamma\gamma$

The effective interaction of Eq. (A14) allows us to estimate the rates for $K \to \pi\gamma\gamma$. Using the matrix elements of the current operator (3.1),

$$\begin{aligned}\sqrt{2}\,\langle \pi^0(q)|J_\mu^0|K^0(p)\rangle &= -\sqrt{2}\,\langle \pi^0(q)|J_\mu^{0\dagger}|\bar{K}^0(p)\rangle \\ &= \langle \pi^+(q)|J_\mu^0|K^+(p)\rangle \\ &= [(p+q)_\mu f_+(t) \\ &\quad + (p-q)_\mu f_-(t)], \\ &\quad t = (p-q)^2 \end{aligned} \tag{3.20}$$

we obtain

$$\begin{aligned} &T(K_L \to \pi^0\gamma\gamma) = 0, \\ &iT(K^+ \to \pi^+\gamma\gamma) = iT(K_S \to \pi^0\gamma\gamma) \\ &= -i\frac{G_F}{\sqrt{2}}\frac{2\alpha}{\pi}\cos\theta_C \sin\theta_C Q^2\left[F\left(\frac{m_\phi^2}{t}\right) - F\left(\frac{m_{\phi'}^2}{t}\right)\right]\epsilon^\rho \epsilon^\sigma \frac{2}{t}\Lambda_{\rho\sigma\mu}[(p+q)^\mu f_+(t) + (p-q)^\mu f_-(t)], \end{aligned} \tag{3.21}$$

where $\Lambda_{\rho\sigma\mu}$ is defined in Appendix A. The decay rate is proportional to the square of the divergence form factor

$$f(t) = f_+(t) + \frac{t}{m_K^2 - m_\pi^2} f_-(t).$$

In these decays the momentum transfer squared t varies from 0 to $(m_K - m_\pi)^2 \simeq 0.53 m_K^2$. Assuming that in this range $f(t) \simeq f(0)$, and $F(m_\phi^2/t) = F$ = constant, we have

$$\begin{aligned}\Gamma(K_S \to \pi\gamma\gamma) &= \frac{1}{2m_K} m_K^4\left[\frac{G_F}{\sqrt{2}}\frac{4\alpha}{\pi}Q^2\cos\theta_C \sin\theta_C F f_+(0)\right]^2 \\ &\quad \times \frac{m_K^2}{64(2\pi)^3}\int_0^{0.53} dx(1-x). \end{aligned} \tag{3.22}$$

To eliminate F, we take the ratio $\Gamma(K_S \to \pi\gamma\gamma)/\Gamma(K_L \to \gamma\gamma)$:

$$\begin{aligned}\frac{\Gamma(K_S \to \pi\gamma\gamma)}{\Gamma(K_L \to \gamma\gamma)} &\simeq \frac{m_K^2 f_+^2(0)}{f_K^2}\frac{1}{32\pi^2}\int_0^{0.53} dx(1-x) \\ &\simeq 10^{-2}. \end{aligned} \tag{3.23}$$

The above estimate does not take into account the fact that $F(t_0/t)$ vanishes as $t \to 0$. Depending on t_0, the ratio of (3.23) may be much smaller, say $\simeq 10^{-3}$.

Note that the estimates of (3.21) for $K_L \to \pi^0\gamma\gamma$ and $K_S \to \pi^0\gamma\gamma$ are consistent with the soft-pion theorems one can derive which connect the real parts of these amplitudes to those of $K_S \to \gamma\gamma$ and $K_L \to \gamma\gamma$. The derivation of these soft-pion theorems is analogous to that given in Sec. II B, and is based on the fact that the relevant part of the weak-interaction Lagrangian $\mathfrak{L}_W$ and the electromagnetic current j_μ^γ commute with the right-handed chiral charge $Q^3 + Q_5^3$, in the limit of the chiral SU(2) symmetry. There is no analogous relation for $K^+ \to \pi^+\gamma\gamma$ and $K \to \gamma\gamma$ because j_μ^γ does not commute with $Q^\pm + Q_5^\pm$. Nevertheless, we see no reason why the amplitude for $K^+ \to \pi^+\gamma\gamma$ should be suppressed, and we expect its order of magnitude to be given correctly by (3.21). In reality, $K_L \to \pi^0\gamma\gamma$ can proceed through the 3π intermediate states by the sequence $K_L \to \pi^0(\pi^+\pi^-) \to \pi^0(\gamma\gamma)$. Again, as for $K_S \to \gamma\gamma$, we interpret the quark-model result to mean that the dispersive part of the $K_L \to \pi^0\gamma\gamma$ amplitude is of order ϵ compared to the $K_S \to \pi^0\gamma\gamma$ amplitude. We have estimated the unitarity correction to $K_L \to \pi^0\gamma\gamma$ and found it negligible.[21]

D. $K \to \pi e\bar{e}$

The effective $\lambda\mathfrak{N}\gamma$ vertex evaluated in Appendix D allows us to evaluate the rates for $K \to \pi e\bar{e}$. By far the largest contribution to the amplitude comes

from the transition charge-radius term in the effective $\lambda\mathfrak{N}\gamma$ vertex (see Appendix D):

$$\bar{\mathfrak{N}}[\,\Gamma_\mu^{(\gamma)}(p-\tfrac{1}{2}k,\,p+\tfrac{1}{2}k)]_{\text{renormalized}}\,\lambda$$
$$=\bar{\mathfrak{N}}\gamma^\nu[\tfrac{1}{2}(1-\gamma_5)]\,\lambda(k^2 g_{\nu\mu}-k_\nu k_\mu)\tfrac{1}{6}\langle r^2\rangle_{\mathfrak{N}\lambda}+\cdots, \tag{3.24}$$

$$\tfrac{1}{6}\langle r^2\rangle_{\mathfrak{N}\lambda}=-Q\,\frac{e}{6\pi^2}\,\frac{G_F}{\sqrt{2}}\cos\theta_C\sin\theta_C\ln\frac{m_{\mathcal{P}'}{}^2}{m^2}, \tag{3.25}$$

where m is the typical uncharmed hadron mass scale.

The computation of Eq. (3.25) is outlined in Appendix D. Briefly, it comes about in the following way. To lowest order in $m_W{}^{-2}$, the charge radius comes from the diagrams shown in Fig. 9(a). After the Fierz-Michel rearrangement of Sec. III A, one sees that the sum of the $\mathcal{P}$- and $\mathcal{P}'$-quark diagrams are convergent and gauge-invariant, even after the replacement

$$ig_{\mu\nu}\frac{g^2}{r^2-m_W{}^2}\to ig_{\mu\nu}\frac{g^2}{m_W{}^2}=ig_{\mu\nu}8\,\frac{G_F}{\sqrt{2}} \tag{3.26}$$

is made. In this limit the relevant diagrams reduce to those of Fig. 9(b), precisely those of the current-current theory modified by the GIM mechanism. Since the mass of the unknown quark appears only through a logarithm, Eq. (3.25) may be expected to be rather stable against uncertainties due to strong interactions.

The amplitudes for $K\to\pi e\bar{e}$ are

$$iT(K^+(p)\to\pi^+(q)e\bar{e})=iT(K_s(p)\to\pi^0(q)e\bar{e})$$
$$=i\,\frac{G_F}{\sqrt{2}}\,\frac{2\alpha}{3\pi}\,\delta\cos\theta_C\sin\theta_C$$
$$\times(p+q)_\mu f_+(t)\bar{e}\gamma^\mu e, \tag{3.27}$$
$$T(K_L\to\pi^0 e\bar{e})=0,$$
$$\delta=Q\ln\frac{m_{\mathcal{P}'}{}^2}{m^2},$$

which give

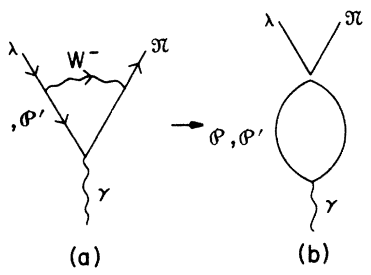

FIG. 9. Leading contribution to the $\lambda\mathfrak{N}$ transition charge radius.

$$\frac{\Gamma(K^+\to\pi^+e\bar{e})}{\Gamma(K^+\to\pi^0\bar{e}\nu)}=\frac{2\Gamma(K_S\to\pi^0e\bar{e})}{\Gamma(K_L\to\pi e\nu)}$$
$$=\left(\frac{2\alpha}{3\pi}\,\delta\cos\theta_C\right)^2. \tag{3.28}$$

[The difference of the factor 2 between (2.12) and (3.28) is due to the difference in the lepton couplings: $\bar{\nu}\gamma^\mu(1-\gamma_5)\nu$ for the former, $\bar{e}\gamma^\mu e$ for the latter.] Taking $\delta=\frac{2}{3}\ln(m_{\mathcal{P}'}/m)^2\simeq 5$ (2), we find that

$$\frac{\Gamma(K^+\to\pi^+e\bar{e})}{\Gamma(K^+\to\text{all})}\simeq 3\times10^{-6}\ (0.5\times10^{-6}), \tag{3.29}$$

$$\frac{\Gamma(K_S\to\pi^0e\bar{e})}{\Gamma(K_L\to\text{all})}\simeq 10^{-8}\ (0.2\times10^{-8}). \tag{3.30}$$

The experimental upper bound[22]

$$\left[\frac{\Gamma(K^+\to\pi^+e\bar{e})}{\Gamma(K^+\to\text{all})}\right]_{\text{exp}}\lesssim(0.4\times10^{-6})$$

is at the verge of contradicting the prediction (3.29).

As for the process $K_L\to\pi^0e\bar{e}$, one-photon- and Z-exchange diagrams are absent by CP invariance; the W^+W^- contribution is expected to be strongly suppressed as for the process $K_L\to\pi^0\nu\bar{\nu}$.

IV. CONCLUDING REMARKS

We summarize in Table I (see Refs. 5, 6, 22–24) the main results of the present study and compare them to experiment. Owing to the extreme experimental difficulties in carrying out the necessary precision, the predictions of our treatment of the Weinberg-Salam model are well within the presently available experimental upper bounds in most cases. A notable exception is in the rate of $K^+\to\pi^+e\bar{e}$, where the experimental upper bound appears tantalizingly close to the limit of a reasonable range of theoretical uncertainties. We feel that the estimate (3.29) is of good standing; deviation of the experimental rate by a decade, say, would worry us. Measurement of this rate, not just setting of an upper bound, is clearly called for.

In most gauge models proposed so far, we believe that most of the results of this paper are also true.

(1) In the eight-quark version of the Georgi-Glashow model, most of the results on semileptonic decays also hold, as shown by Lee, Primack, and Treiman, and Lee and Treiman.[25] For electromagnetic decays, the situation is murky. This is due to two factors. One is that in this model there might be an important contribution of the physical Higgs scalar to strangeness-changing transitions which we have not considered in this paper. The second is that in this model the $\lambda\mathfrak{N}$

TABLE I. The result of this investigation. The parameter ϵ is the GIM suppression factor. Depending on the relevant Feynman integrals, this parameter is either of order $(|\Delta m^2|/m_W^2 \sin^2\theta)\ln(m_W^2/m_{\phi'}^2)$ or order $|\Delta m^2|/(m_W^2 \sin^2\theta)$. In this table we take ϵ to be 10^{-2}.

Process	Order of magnitude of the amplitude	Order of magnitude of branching ratio	Experimental rate or bound [e]	Comments
$K_L^0 \to \mu\bar{\mu}$	$G_F\alpha^2$	10^{-8}	10^{-8} (Ref. 5)	see text
$K_S^0 \to \mu\bar{\mu}$	$G_F\alpha^2$	10^{-10}	$<3.1\times10^{-7}$ (Ref. 23)	
$K^+ \to \pi^+\nu\bar{\nu}$	$G_F\alpha\epsilon$	10^{-10}	$<5.6\times10^{-7}$ (Ref. 24)	
$K_L^0 \to \pi^0\nu\bar{\nu}$	forbidden		...	see text
$K_S^0 \to \pi^0\nu\bar{\nu}$	$G_F\alpha\epsilon$	10^{-12}	...	
$K_L \to \gamma\gamma$	$G_F\alpha$	10^{-4}	$(4.9\pm0.4)\times10^{-4}$	input
$K_S \to \gamma\gamma$	$G_F\alpha$	$\sim1.4\times10^{-6}$	$<0.7\times10^{-3}$	a, b
$K^+ \to \pi^+\gamma\gamma$	$G_F\alpha$	10^{-6}–10^{-7}	$<3.5\times10^{-5}$	
$K_L^0 \to \pi^0\gamma\gamma$	$G_F\alpha\epsilon$	$<10^{-7}$	$<2.4\times10^{-4}$	b, c
$K_S^0 \to \pi^0\gamma\gamma$	$G_F\alpha$	10^{-8}–10^{-9}	...	b, d
$K^+ \to \pi^+ e\bar{e}$	$G_F\alpha$	10^{-6}	$<0.4\times10^{-6}$ (Ref. 22)	
$K_L^0 \to \pi^0 e\bar{e}$	strongly suppressed		...	see text
$K_S^0 \to \pi^0 e\bar{e}$	$G_F\alpha$	10^{-8}	...	

[a] The 2π contribution gives $\Gamma(K_S \to \gamma\gamma) \sim 2\times10^4\ \text{sec}^{-1}$.
[b] Not clear in the Georgi-Glashow model.
[c] $\Gamma(K_L \to \pi^0\gamma\gamma)/\Gamma(K_S \to \pi^0\gamma\gamma) \lesssim 10^{-4}$.
[d] $\Gamma(K_S \to \pi\gamma\gamma)/\Gamma(K_L \to \gamma\gamma) \simeq 10^{-2}$ or 10^{-3}.
[e] Unless otherwise noted these numbers are taken from the Particle Data Group (Ref. 6).

transition magnetic moment is large, being of the order of[26]

$$[\mathfrak{M}_{\lambda\mathfrak{N}}]_{GG} = O\left(\frac{G_F}{\sqrt{2}}\, e(m_{\mathfrak{N}} + m_\lambda) m_{\phi'} \sin\theta_C\right).$$

[This is analogous to the anomalous magnetic moment of the muon in this model. It is of the order of $(G_F/\sqrt{2})e m_\mu m(Y^+)$.] We do not know of a way of assessing the effects of the transition moment in the $K \to \pi$ transitions reliably.

(2) In the Bars-Halpern-Yoshimura model,[27] almost all of the present results should hold also. The reason is this: Since this model incorporates the field algebra, most integrals one encounters are superconvergent, so much so that they remain so even when the replacement (3.26) is made. The remaining integral is scaled by the typical hadronic mass m. Thus the integral has the dependence on m_W^{-2}, as a naive counting of the number of heavy boson propagators indicates: We expect the amplitude for $K_L \to \mu\bar{\mu}$ to be of order $G_F\alpha(m/m_W)^2$; the amplitudes for $K_L \to \gamma\gamma$ of order $G_F\alpha$, etc.

(3) The situation in the Lee-Prentki-Zumino (LPZ) model[28] should be almost identical to that in the Weinberg-Salam model.

ACKNOWLEDGMENT

We have benefited from conversations with D. Cline, J.-M. Gaillard, S. L. Glashow, R. H. Hildebrand, T. D. Lee, J. Rosner, L. M. Sehgal, J. Smith, S. B. Treiman, and S. Weinberg.

APPENDIX A: FREE-QUARK MATRIX ELEMENTS

In this appendix, we collect the relevant matrix elements used in the text. These are the expressions correct to lowest order in m_W^{-2}. The derivations are relegated to other appendixes. In the following all calculations are done in the 't Hooft–Feynman gauge.[9]

(1). The effective $\mathfrak{N}\lambda Z$ vertex:

$$iE_\mu^{(2)}(q,p) = \bar{\mathfrak{N}}(q)\gamma_\mu[\tfrac{1}{2}(1-\gamma_5)]\lambda(p) \times \{i(g^2+g'^2)^{1/2}\cos\theta_C \sin\theta_C(\alpha/8\pi) \times \epsilon_0[\ln(m_W/m_{\phi'})^2 - 1]\}, \quad \text{(A1)}$$

where $\epsilon_0 = \Delta m^2/m_W^2 \sin^2\theta_W$, $\Delta m^2 = m_{\phi'}^2 - m_\phi^2$.

(2). The Z-meson propagator:

$$-i g_{\mu\nu}\frac{1}{k^2 - m_Z^2} \simeq i g_{\mu\nu}\frac{4}{(g^2+g'^2)v^2}, \quad \text{(A2)}$$

where v is the vacuum expectation value of the Higgs scalar field.

(3). The Z^0-meson couplings to leptons:

$$\mathcal{L}_{Zll} = (g^2+g'^2)^{1/2}\,(\nu_\mu \tfrac{1}{2}\gamma^\alpha[\tfrac{1}{2}(1-\gamma_5)]\nu_\mu + \bar{\mu}\gamma^\alpha\{-\tfrac{1}{2}[\tfrac{1}{2}(1-\gamma_5)]-\sin^2\theta_W\}\mu), \tag{A3}$$

and similarly for the electronic leptons.

(4). The effective $\gamma\lambda\mathfrak{N}$ vertex:

$$iE_\mu^{(\gamma)}(q,p) = \bar{\mathfrak{N}}(q)\gamma_\mu[\tfrac{1}{2}(1-\gamma_5)]\lambda(p) i\,\frac{eQ}{\pi^2}\,\frac{G}{\sqrt{2}}\cos\theta_C \times (k^2 g_{\nu\mu}-k_\nu k_\mu)F(k^2, m_{\mathcal{P}}^2, m_{\mathcal{P}'}^2) \tag{A4}$$

where $m_{\mathcal{P}}$ and $m_{\mathcal{P}'}$ are the masses of the $\mathcal{P}$- and $\mathcal{P}'$-type quarks of charge Q, respectively, and

$$F(k^2,a,b) = \int_0^1 dz\, z(1-z)\ln\frac{b-k^2z(1-z)}{a-k^2z(1-z)}. \tag{A5}$$

$G = 1/2v^2 = g^2/8m_W^2$ is the Fermi coupling constant.

(5). The irreducible $ll\lambda\mathfrak{N}$ vertex:

$$iS = \bar{\mathfrak{N}}\gamma^\alpha[\tfrac{1}{2}(1-\gamma_5)]\lambda\{-4\bar{\nu}\gamma_\alpha[\tfrac{1}{2}(1-\gamma_5)]\nu+\bar{\mu}\gamma_\alpha[\tfrac{1}{2}(1-\gamma_5)]\mu\}(-\tfrac{1}{2}i)\,\frac{G}{\sqrt{2}}\,\frac{\alpha}{\pi}\cos\theta_C\sin\theta_C\left[\frac{\Delta m^2}{m_W^2\sin^2\theta_W}\left(\ln\frac{m_W^2}{m_{\mathcal{P}'}^2}-1\right)\right]. \tag{A6}$$

The sum of the box diagram and the Z-exchange diagram for $\lambda\bar{\mathfrak{N}}\to\bar{l}l$:

$$\simeq i\,\frac{G}{\sqrt{2}}\,\frac{\alpha}{\pi}\cos\theta_C\sin\theta_C\,\frac{\Delta m^2}{m_W^2\sin^2\theta_W} \times \ln\frac{m_W^2}{m_{\mathcal{P}'}^2}\,\bar{\mathfrak{N}}\gamma_\alpha[\tfrac{1}{2}(1-\gamma_5)]\lambda \times\{\bar{\mu}\gamma^\alpha\mu\sin^2\theta_W+\tfrac{3}{2}\bar{\nu}\gamma^\alpha[\tfrac{1}{2}(1-\gamma_5)]\nu\}. \tag{A7}$$

(6). Two-photon modes:

$$iT_{\rho\sigma} = i\,\frac{G_F}{\sqrt{2}}\cos\theta_C\sin\theta_C\,\bar{\mathfrak{N}}\gamma^\mu(1-\gamma_5)\lambda\,\frac{e^2}{(2\pi)^4}R_{\rho\sigma\mu}Q^2, \tag{A8}$$

where $R_{\rho\sigma\mu}$ is the quantity defined by Rosenberg and Adler,[19] except that we associate ρ with the photon with momentum k_1 and σ with k_ν:

$$R_{\rho\sigma\mu}(k_1,k_2) = [k_{1\sigma}\epsilon_{\alpha\beta\rho\mu}k_1^\alpha k_2^\beta - k_{2\rho}\epsilon_{\alpha\beta\sigma\mu}k_1^\alpha k_2^\beta + (k_1\cdot k_2)\epsilon_{\alpha\rho\sigma\mu}(k_1-k_2)^\alpha]A_3 \equiv \Lambda_{\rho\sigma\mu}A_3, \tag{A9}$$

where

$$A_3 = -16\pi^2\left[\int_0^1 dx\int_0^{1-x} dy\,\frac{xy}{2xyk_1\cdot k_2 - m_p^2} - (m_{\mathcal{P}}^2\to m_{\mathcal{P}'}^2)\right]. \tag{A10}$$

The expressions (A9), (A10) are valid for real photons.

The form factor $A_3(s)$, $s = 2k_1\cdot k_2$, may be simplified:

$$A_3(s) = -16\pi^2\,\frac{1}{s}\left[F\left(\frac{m_{\mathcal{P}}^2}{s}\right) - F\left(\frac{m_{\mathcal{P}'}^2}{s}\right)\right], \tag{A11}$$

where

$$F(\beta) = \tfrac{1}{2}+\beta\int_0^1\frac{dx}{x}\ln\left[1-\frac{x(1-x)}{\beta}\right] \tag{A12}$$

and has the asymptotic behavior

$$F(\beta)\to -\frac{1}{24\beta}, \quad \beta\gg 1 \qquad \to \tfrac{1}{2}, \quad \beta\ll 1. \tag{A13}$$

The part of (A8) relevant to $K_L\to\gamma\gamma$ may be written as

$$iT_{\rho\sigma} = -i\,\frac{G_F}{\sqrt{2}}\,\frac{\alpha}{\pi}\,Q^2\cos\theta_C\sin\theta_C\,\bar{\mathfrak{N}}\gamma^\mu(1-\gamma_5)\lambda \times 4\frac{1}{s}\left[F\left(\frac{m_{\mathcal{P}}^2}{s}\right)-F\left(\frac{m_{\mathcal{P}'}^2}{s}\right)\right]\tfrac{1}{2}s\epsilon_{\alpha\rho\sigma\mu}(k_1-k_2)^\alpha. \tag{A14}$$

APPENDIX B: THE EFFECTIVE $\gamma\mathfrak{N}Z$ VERTEX

In lowest order the effective $\lambda\mathfrak{N}Z$ vertex is generated by the diagrams shown in Fig. 10(a)–

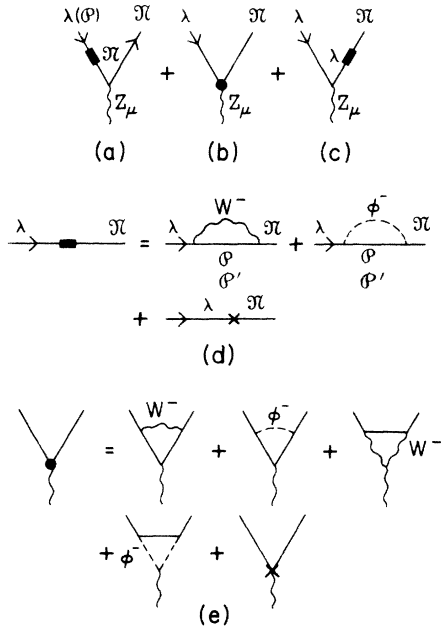

FIG. 10. Diagrams contributing to the effective $\lambda\mathfrak{N}Z$ vertex.

10(c). The off-diagonal mass matrix element $\Sigma(p)$ and the irreducible $\lambda\mathfrak{N}Z$ vertex $\Gamma_\mu^{(Z)}(q,p)$ are depicted in Fig. 10(d) and Fig. 10(e), respectively. The crosses in Fig. 10 represent the contributions of counterterms.

The renormalization counterterms arise in the following way. We renormalize the left-chiral fermion fields according to

$$\begin{pmatrix} \mathcal{P}_u \\ \mathfrak{N}_u' \end{pmatrix}_L = Z_L^{1/2} \begin{pmatrix} \mathcal{P} \\ \mathfrak{N}' \end{pmatrix}_L ,$$

$$\begin{pmatrix} \mathcal{P}_u' \\ \lambda_u' \end{pmatrix}_L = Z_L'^{1/2} \begin{pmatrix} \mathcal{P}' \\ \lambda' \end{pmatrix}_L ,$$

and similarly for the right-handed fermion fields, and renormalize coupling constants and gauge bosons according to

$$g_u = g \frac{Z_1}{Z_L Z_3^{1/2}} ,$$

$$g_u' = g' \frac{Z_1'}{Z_L Z_3'^{1/2}} ,$$

$$A_{u\mu}^3 = A_\mu^3 Z_3^{1/2} ,$$

$$B_{u\mu} = B_\mu Z_3'^{1/2} ,$$

and choose the renormalization constants by suitably chosen conventions. We define the Weinberg angle in terms of renormalized constants:

$$\cos\theta_W = g/(g^2+g'^2)^{1/2} .$$

The relevant counterterms in Figs. 10(d) and 10(e) then take the form

$$\bar{\mathfrak{N}}\left[\tfrac{1}{2}(1-\gamma_5)\right]\{i\gamma\cdot\partial-(g^2+g'^2)^{1/2}[-\tfrac{1}{2}-(Q-1)\sin^2\theta_W]\gamma\cdot Z\}\lambda\cos\theta_C\sin\theta_C(Z_L-Z_L') , \tag{B1}$$

to lowest order; the term $Z_L - Z_L'$ is convergent, and its finite part may be so adjusted as to cancel the $\lambda\to\mathfrak{N}$ transition on mass shell.

Straightforward evaluation of diagrams, Figs. 10(a)–10(c), is not difficult and has been performed. When $\lambda(p)$ and $\mathfrak{N}(q)$ are on the mass shell, the use of the Ward-Takahashi identity connecting Γ_μ and Σ simplifies the calculation considerably:

$$(q-p)^\mu\Gamma_\mu^{(Z)}(q,p)-[\Sigma(q)T-T^*\Sigma(p)] + i(-\tfrac{1}{2})(g^2+g'^2)^{1/2}v\Gamma_2(q,p)=0 , \tag{B2}$$

where Γ_2 is the irreducible $\mathfrak{N}\lambda\phi_2$ vertex (see Fig. 11). This follows from the Ward-Takahashi identities for proper vertices[29] in the one-loop approximation, where the effects of the Feynman-DeWitt-Faddeev-Popov ghost fields may be neglected. Alternatively it may be derived by the current-algebra technique applied to the source current of the Z meson. In (B2) the matrix T is

$$T=\{[-\tfrac{1}{2}-(Q-1)\sin^2\theta_W]L-(Q-1)\cos^2\theta_W R\} \times(g^2+g'^2)^{1/2} , \quad L=[\tfrac{1}{2}(1-\gamma_5)] , \quad [\tfrac{1}{2}(1+\gamma_5)] \quad T^*=\gamma_0 T^\dagger\gamma_0 . \tag{B3}$$

To order g^4, $g\sim e$, and to lowest order in (m_h^2/m_W^2), the vertices $\Gamma_\mu^{(Z)}$ and Σ have the kinematical structure

$$\Gamma_\mu^{(Z)}(q,p)=\gamma_\mu Lx , \quad \Sigma(p)=\gamma\cdot pLa+bL+cR \tag{B4}$$

when one assumes $m_\mathcal{P}\simeq m_\mathfrak{N}\simeq m_\lambda \ll m_{\mathcal{P}'}$. The effective $\lambda\mathfrak{N}Z$ vertex is then

$$i\bar{u}_\mathfrak{N}(q)E_\mu^{(Z)}u_\lambda(p)=\bar{u}_\mathfrak{N}(q)\left[i\Gamma_\mu^{(Z)}+i\gamma_\mu T\frac{i}{\not p-m_n}i\Sigma(\not p) + i\Sigma(q)\frac{i}{\not q-m_\lambda}i\gamma_\mu T\right]u_\lambda(p)$$
$$=i\bar{u}_\mathfrak{N}(q)\gamma_\mu Lu_\lambda(p) \times\{x-[-\tfrac{1}{2}-(Q-1)\sin^2\theta_W]a\} . \tag{B5}$$

On the other hand, we learn from the Ward identity (B2) that Γ_2 is of the form

$$\tfrac{1}{2}i(g^2+g'^2)^{1/2}v\Gamma_2=(q-p)\cdot\gamma L \times\{x+[\tfrac{1}{2}+(Q-1)\sin^2\theta_W]a\} , \tag{B6}$$

so that to evaluate the effective vertex $iE_\mu^{(Z)}$ one needs only to extract the terms in Γ_2 proportional to $(q-p)\cdot\gamma[\frac{1}{2}(1-\gamma_5)]$. In one-loop approximation, Γ_2 receives contributions from diagrams in Fig. 11 and

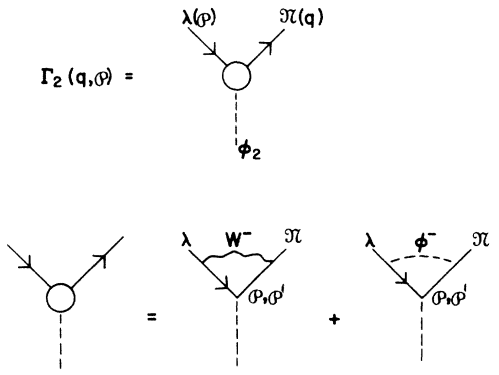

FIG. 11. The $\lambda\mathfrak{N}\phi$ vertex.

$$\Gamma_2(q,p)\cong \tfrac{1}{2}g^2\left[\frac{m_{\mathcal{P}}^2}{v}\cos\theta_C\sin\theta_C\,2(q-p)\cdot\gamma[\tfrac{1}{2}(1-\gamma_5)]\right.$$
$$\times\int\frac{d^4\gamma}{(2\pi)^4}\left(\frac{i}{\gamma^2-m^2}\right)^2\frac{i}{\gamma^2-m_W^2}$$
$$\left.-(m_{\mathcal{P}}\to m_{\mathcal{P}'})\right]\cdots . \qquad \text{(B7)}$$

The above expression is valid as $q-p\to 0$. Thus if $(q-p)^2\ll m_{\mathcal{P}}^2$ or $m_{\mathcal{P}'}^2$, we have

$$E_\mu^{(Z)}=g^2(g^2+g'^2)^{1/2}\cos\theta_C\sin\theta_C\,\bar{\mathfrak{N}}\,\gamma_\mu\tfrac{1}{2}[(1-\gamma_5)]\lambda$$
$$\times\frac{1}{16\pi^2}\,\frac{\Delta m^2}{m_W^2}\left(\ln\frac{m_W^2}{m_h^2}-1\right), \qquad \text{(B8)}$$

where m_h is the larger of $m_{\mathcal{P}}$ and $m_{\mathcal{P}'}$.

Note further that the counterterms exhibited in (B1) do not contribute to the effective vertex on the mass shell in (B5). This is as it should be, since the counterterms in (B1) can be completely eliminated from the Lagrangian if the strong interactions preserve the weak-interaction symmetry.

Equation (B8) refers to on-shell n and λ. The off-shell corrections are of the order p^2/m_W^2, where p is the off-shell momentum.

APPENDIX C: BOX DIAGRAMS FOR THE PROCESS $\lambda+\bar{\mathfrak{N}}\to l+\bar{l}$

In the Weinberg-Salam model there are two diagrams each (see Fig. 12) for $\lambda+\bar{\mathfrak{N}}\to\mu+\bar{\mu}$ and $\lambda+\bar{\mathfrak{N}}\to\nu+\bar{\nu}$. The second diagrams are generated from the first by replacing the $\mathcal{P}$-quark line by the $\mathcal{P}'$. The computation involved is very similar to that of Lee, Primack, and Treiman[25] for the Georgi-Glashow model. The contributions of the diagrams in which one or both of the W lines are replaced by the unphysical Higgs scalars may be safely neglected, since such diagrams are down by at least one power of $(m_L/m_W)^2$.

In the limit of neglecting external momenta compared to the internal one we have

$$iS(\lambda+\bar{\mathfrak{N}}\to\mu+\bar{\mu})$$
$$=\tfrac{1}{4}g^4\left[\int\frac{d^4\gamma}{(2\pi)^4}\left(\bar{\mathfrak{N}}\gamma^\rho[\tfrac{1}{2}(1-\gamma_5)]\,\frac{i}{\gamma\cdot\gamma-m_{\mathcal{P}}}\,\gamma^\sigma[\tfrac{1}{2}(1-\gamma_5)]\lambda\right)\{\bar{\mu}\,\gamma_\sigma[\tfrac{1}{2}(1-\gamma_5)]\,\frac{i}{\gamma\cdot\gamma}\,\gamma_\rho\mu\}\left(\frac{-i}{\gamma^2-m_W^2}\right)^2-(m_{\mathcal{P}}\to m_{\mathcal{P}'})\right],$$
$$\text{(C1)}$$

$$iS(\lambda+\bar{\mathfrak{N}}\to\nu+\bar{\nu})$$
$$=\tfrac{1}{4}g^4\left[\int\frac{d^4\gamma}{(2\pi)^4}\left(\bar{\mathfrak{N}}\gamma^\rho[\tfrac{1}{2}(1-\gamma_5)]\,\frac{i}{\gamma\cdot\gamma-m_{\mathcal{P}}}\,\gamma^\sigma[\tfrac{1}{2}(1-\gamma_5)]\lambda\right)\left(\bar{\nu}\,\gamma_\rho[\tfrac{1}{2}(1-\gamma_5)]\,\frac{i}{-\gamma\cdot\gamma}\,\gamma_\sigma\nu\right)\left(\frac{-i}{\gamma^2-m_W^2}\right)^2-(m_{\mathcal{P}}\to m_{\mathcal{P}'})\right],$$
$$\text{(C2)}$$

where we have neglected the muon mass. The Dirac algebra can be simplified by

$$\gamma^\rho\gamma^\alpha\gamma^\sigma=g^{\rho\alpha}\gamma^\sigma+g^{\alpha\sigma}\gamma^\rho-g^{\rho\sigma}\gamma^\alpha-i\epsilon^{\rho\alpha\sigma\beta}\gamma_5\gamma_\beta,$$
$$\epsilon^{\rho\alpha\sigma\beta}\gamma_\sigma\gamma_\alpha\gamma_\rho=-6i\gamma_5\gamma^\beta,$$

and

$$\{\gamma^\rho\gamma^\alpha\gamma^\sigma[\tfrac{1}{2}(1-\gamma_5)]\}\{\gamma_\sigma\gamma_\alpha\gamma_\rho[\tfrac{1}{2}(1-\gamma_5)]\}$$
$$=4\{\gamma^\alpha[\tfrac{1}{2}(1-\gamma_5)]\}\{\gamma_\alpha[\tfrac{1}{2}(1-\gamma_5)]\}$$
$$\{\gamma^\rho\gamma^\alpha\gamma^\sigma[\tfrac{1}{2}(1-\gamma_5)]\}\{\gamma_\rho\gamma_\alpha\gamma_\sigma[\tfrac{1}{2}(1-\gamma_5)]\} \qquad \text{(C3)}$$
$$=16\{\gamma^\alpha[\tfrac{1}{2}(1-\gamma_5)]\}\{\gamma_\alpha[\tfrac{1}{2}(1-\gamma_5)]\}.$$

The resulting expressions are

$$iS\left(\lambda+\bar{\mathfrak{N}}\to\begin{matrix}\mu+\bar{\mu}\\ \nu+\bar{\nu}\end{matrix}\right)=-i\begin{pmatrix}1\\ -4\end{pmatrix}\frac{g^4}{64\pi^2m_W^2}\{\bar{\mathfrak{N}}\gamma^\alpha[\tfrac{1}{2}(1-\gamma_5)]\lambda\}\{\bar{l}\,\gamma_\alpha[\tfrac{1}{2}(1-\gamma_5)]\,l\}\int_0^\infty\frac{x\,dx}{(x+1)^2}\left(\frac{1}{x+y}-\frac{1}{x+y'}\right),$$

where

$$y=m_{\mathcal{P}}^2/m_W^2, \text{ and } y'=m_{\mathcal{P}'}^2/m_W^2.$$

APPENDIX D: THE EFFECTIVE $\lambda\mathfrak{N}\gamma$ VERTEX

If we write the irreducible $\lambda\mathfrak{N}\gamma$ vertex as $\Gamma_\mu^{(\gamma)}(q,p)$, the effective $\lambda\mathfrak{N}\gamma$ vertex $E_\mu^{(\gamma)}(q,p)$ defined similarly to $E_\mu^{(z)}(q,p)$, i.e., by the sum of three diagrams [Figs. 10(a)–10(c)], where the Z line is replaced by the photon line, is

$$E_\mu^{(\gamma)}=\Gamma_\mu^{(\gamma)}-e(Q-1)\gamma_\mu La, \qquad \text{(D1)}$$

where a is defined in (B4). The usual Ward identity states

$$(q-p)^\mu\Gamma_\mu^{(\gamma)}(q,p)=e(Q-1)[\Sigma(q)-\Sigma(p)]. \qquad \text{(D2)}$$

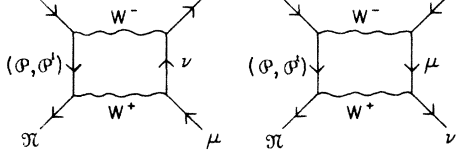

FIG. 12. Irreducible $\lambda\bar{\mathfrak{N}}l\bar{l}$ vertex.

The proper vertex may be expanded in powers of external momenta. The structures of (D2) and (B4) restrict it to be of the form

$$\Gamma_\mu^{(\gamma)}(p-\tfrac{1}{2}k, p+\tfrac{1}{2}k) = e(Q-1)\gamma_\mu L a + i\sigma_{\mu\nu}k^\nu(m_{\mathfrak{N}}+m_\lambda)^{-1}\mathfrak{M}_{\mathfrak{N}\lambda} + \gamma^\nu(k^2 g_{\mu\nu}-k_\nu k_\mu)\tfrac{1}{6}\langle r^2\rangle_{\mathfrak{N}\lambda} L + \cdots, \quad \text{(D3)}$$

where higher-order terms in external momenta are neglected. Thus the effective photon vertex $E_\mu^{(\gamma)}$ of (D1) consists of two terms—the transition magnetic-moment term $\mathfrak{M}_{\lambda\mathfrak{N}}$ and the transition charge-radius term $\frac{1}{6}\langle r^2\rangle_{\mathfrak{N}\lambda}$. We shall compute them in turn. The diagrams contributing to $\Gamma_\mu^{(\gamma)}$ are shown in Fig. 13.

The computation of the transition magnetic moment proceeds very similarly to that of the weak contribution to the muon anomalous moment in the Weinberg-Salam model. Figures 13(a) and 13(b) are nonexistent for the muon anomalous moment, since the neutrino is electrically neutral. Figure 13(a) contributes to the transition magnetic moment (in the 't Hooft–Feynman gauge):

$$\mathfrak{M}_{\mathfrak{N}\lambda}^{(a)} = -eQ\frac{G_F}{\sqrt{2}}\frac{1}{8\pi^2}(m_{\mathfrak{N}}+m_\lambda)^2\tfrac{1}{2}\left(1+\gamma_5\frac{m_\lambda-m_{\mathfrak{N}}}{m_\lambda+m_{\mathfrak{N}}}\right)\times\left(\frac{\Delta m^2}{m_W^2}\ln\frac{m_W^2}{m_{\varphi'}^2}\right)\cos\theta_C\sin\theta_C,$$

and Fig. 13(b) does not. Figures 13(e) and 13(f) do not contribute to the transition magnetic moment, and the contributions of Figs. 13(c) and 13(d) are of the order of

$$\mathfrak{M}_{\mathfrak{N}\lambda}^{(c),(d)} = O\left(e\frac{G_F}{8\pi^2\sqrt{2}}(m_{\mathfrak{N}}+m_\lambda)^2\frac{\Delta m^2}{m_W^2}\cos\theta_C\sin\theta_C\right)$$

without the logarithmic factor $\ln(m_W^2/m_{\varphi'}^2)$.

In the 't Hooft–Feynman gauge, the leading contribution to the transition charge radius comes from Fig. 13(a). This could have been guessed at by a dispersion-theoretic argument and an estimate of coupling strengths. To lowest order in $1/m_W^2$, the W exchange may be replaced by a V-A four-fermion interaction. In this limit we have

$$(ieQ)\frac{(-iG_F)}{\sqrt{2}}\cos\theta_C\sin\theta_C[\bar{\mathfrak{N}}\gamma_\nu(1-\gamma_5)\lambda]\times\left[\mathrm{Tr}\int\frac{d^4r}{(2\pi)^4}\gamma^\nu\frac{i}{(r+\frac{1}{2}k)\cdot\gamma-m_\varphi}\gamma_\mu\times\frac{i}{(r-\frac{1}{2}k)\cdot\gamma-m_\varphi}-(m_\varphi\to m_{\varphi'})\right].$$

The integral to be evaluated is exactly the same as for the vacuum polarization in quantum electrodynamics,[30] so that we get

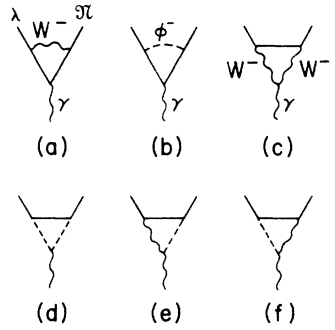

FIG. 13. Diagrams for the $\lambda\mathfrak{N}\gamma$ vertex $\Gamma_\mu^{(\gamma)}$.

$$Q\frac{eG_F}{\sqrt{2}}\cos\theta_C\sin\theta_C[\bar{\mathfrak{N}}\gamma_\nu(1-\gamma_5)\lambda](k_\mu k_\nu - k^2 g_{\mu\nu})\times\frac{i}{2\pi^2}\int_0^1 dZ\,Z(1-Z)\ln\frac{m_{\varphi'}^2-k^2Z(1-Z)}{m_\varphi^2-k^2Z(1-Z)}.$$

Thus

$$\tfrac{1}{6}\langle r^2\rangle_{\mathfrak{N}\lambda} = -eQ\frac{G_F}{\sqrt{2}}\cos\theta_C\sin\theta_C\frac{1}{\pi^2}\times\int_0^1 dZ\,Z(1-Z)\ln\frac{m_{\varphi'}^2-k^2Z(1-Z)}{m_\varphi^2-k^2Z(1-Z)}.$$

For $m_{\varphi'}^2 \gg k^2 \simeq m_k^2 \gg m_\varphi^2$,

$$\tfrac{1}{6}\langle r^2\rangle_{\mathfrak{N}\lambda} \simeq -Q\frac{e}{6\pi^2}\frac{G_F}{\sqrt{2}}\ln\frac{m_{\varphi'}^2}{m_k^2}\cos\theta_C\sin\theta_C.$$

APPENDIX E: IRREDUCIBLE VERTEX FOR $\lambda+\bar{\mathfrak{N}}\to\gamma+\gamma$

Different kinds of diagrams representing the irreducible vertex for the process $\lambda+\bar{\mathfrak{N}}\to\gamma+\gamma$ are shown in Fig. 14. Let us first pursue the relative magnitude of each of these diagrams.

Take for example Figure 14(a). After the usual Feynman parametrization the relevant integrals take the form

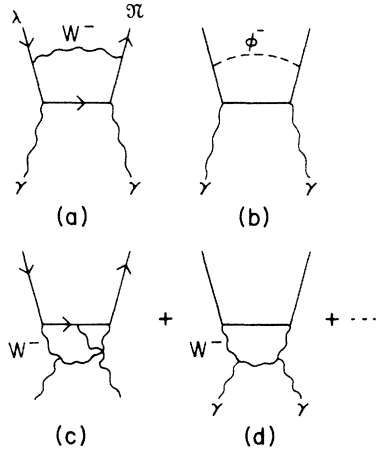

FIG. 14. Some diagrams contributing to the irreducible $\lambda\bar{\mathfrak{N}}\gamma\gamma$ vertex.

$$I_{\alpha\beta\gamma}(p,k_1,k_2)=\int dx_1\,dx_2\,dx_3\,dx_4\,\delta(1-x_1-x_2-x_3-x_4)\int\frac{d^4R}{(2\pi)^4}\,\frac{s_\alpha t_\beta u_\gamma}{[R^2+f(k_1,k_2,p)+x_1m_W{}^2+(x_2+x_3+x_4)m^2]^4}\,,$$

where m is the mass of the internal fermion line; s, t, and u are of the form

$$s_\alpha = R_\alpha + Xk_1 + Yk_2 + Zp\,,$$

X, Y, and Z being linear homogeneous functions of the Feynman parameters $x_1,\ldots,x_4$. The electromagnetic gauge invariance applied to the irreducible vertex states that only the parts of $I_{\alpha\beta\gamma}$ proportional to three powers of external momenta carrying the Lorentz indices α, β, and γ will survive when all diagrams are summed (the argument here is very similar to that of Rosenberg and Adler, except that the presence of an extra momentum p considerably complicates the details, which we do not feel worthy of presenting here), so we need consider only integrals of the form

$$I=\int dx_1\,dx_2\,dx_3\,dx_4\,\delta(1-x_1-x_2-x_3-x_4)\times\frac{1}{[x_1m_W{}^2+(1-x_1)m^2]^2}\,F(x_1,x_2,x_3,x_4) \tag{E1}$$

in the low-energy limit (i.e., $p, k_1, k_2 \to 0$). The integral I in (E1) may appear to be of order $(m_W)^{-4}$ on dimensional grounds, but because of the divergence in the x_1 integration of the form

$$\int\frac{dx_1}{x_1{}^2}$$

when m^2 is neglected, a more careful treatment is called for:

$$\begin{aligned}I&=\frac{1}{m_W{}^4}\int dx_1\,dx_2\,dx_3\,dx_4\,\delta(1-x_1-x_2-x_3-x_4)\times\frac{1}{[x_1+(1-x_1)\epsilon]^2}\,F(x_1,x_2,x_3,x_4)\\&\cong\frac{1}{m_W{}^4}\int\frac{dx_1}{(x_1+\epsilon)^2}\int d\alpha\,d\beta\,d\gamma\,\delta(1-\alpha-\beta-\gamma)\times F(0,\alpha,\beta,\gamma)\\&=\frac{1}{m_W{}^4}\frac{1}{\epsilon}\int d\alpha\,d\beta\,d\gamma\,\delta(1-\alpha-\beta-\gamma)\,F(0,\alpha,\beta,\gamma)\,,\end{aligned} \tag{E2}$$

where $\epsilon=(m/m_W)^2$. Therefore I is of the order of

$$I\simeq O\left(\frac{1}{m_W{}^2}\,\frac{1}{m^2}\right)\,.$$

Similar arguments show the diagrams of the kinds 14(c) and 14(d) are of order $m_W{}^{-4}$, so these can be neglected compared to 14(a). Diagrams such as 14(b), in which a W line is replaced by an unphysical Higgs scalar, are down by a factor of $(m_h/m_W)^2$ compared to the W exchange due to the nature of the couplings involved. Thus, in view of the mass ratio $m_h{}^2/m_W{}^2\ll 1$, the dominant contribution to the *gauge-invariant* part of the irreducible vertex comes from the diagram of Fig. 14(a).

To lowest order in $m_W{}^{-2}$, therefore, the proper vertex for $\lambda+\bar{\mathfrak{N}}\to\gamma+\gamma$ is given by

$$-\left(\frac{ig}{\sqrt{2}}\right)^2(iQe)^2\,\frac{i}{m_W{}^2}\cos\theta_C\sin\theta_C\,\bar{\mathfrak{N}}\,\gamma_\alpha[\tfrac{1}{2}(1-\gamma_5)]\,\lambda\times\left[\left(\mathrm{Tr}\int\frac{d^4\gamma}{(2\pi)^4}\,\gamma^\alpha[\tfrac{1}{2}(1-\gamma_5)]\,\frac{i}{\gamma\!\!\!/+k\!\!\!/_1-m}\,\gamma_\rho\,\frac{i}{\gamma\!\!\!/-m}\,\gamma_\sigma\,\frac{i}{\gamma\!\!\!/-k\!\!\!/_2-m}+(\rho,k_1\to\sigma,k_2)\right)-(m\to m')\right]\,.$$

The integral involved is identical to the one dealt with by Rosenberg and Adler, and the result stated in Appendix A ensues.

APPENDIX F: EFFECTIVE LAGRANGIAN FOR $\lambda+\bar{\mathfrak{N}}\to\mathfrak{N}+\bar{\lambda}$

We write the operator S matrix in the form

$$S=T\exp\left[i\int d^4x\,\mathfrak{L}_1(x)\right]\,, \tag{F1}$$

where the relevant part of the interaction Lagrangian is

$$\begin{aligned}\mathfrak{L}_I=\frac{g}{\sqrt{2}}\{&\bar{\lambda}\gamma_\mu[\tfrac{1}{2}(1-\gamma_5)](\mathcal{P}\sin\theta_C+\mathcal{P}'\cos\theta_C)W^\mu\\&+\bar{\mathfrak{N}}\,\gamma_\mu[\tfrac{1}{2}(1-\gamma_5)](\mathcal{P}\cos\theta_C-\mathcal{P}'\sin\theta_C)W^\mu\\&+\mathrm{H.c.}\}\,.\end{aligned} \tag{F2}$$

The fourth-order term contains

$$\begin{aligned}S_4=+\tfrac{1}{8}g^2(\cos\theta_C\sin\theta_C)^2\int d^4x_1\,d^4x_2\,d^4x_3\,d^4x_4\,(&\bar{\lambda}(x_1)\{\gamma^\mu[\tfrac{1}{2}(1-\gamma_5)]\,iS_F(x_1-x_3;m_{\mathcal{P}})\,\gamma^\beta[\tfrac{1}{2}(1-\gamma_5)]\}\,\mathfrak{N}(x_3)\\&\times\bar{\lambda}(x_2)\{\gamma^\alpha[\tfrac{1}{2}(1-\gamma_5)]\,iS_F(x_2-x_4)\,\gamma^\nu[\tfrac{1}{2}(1-\gamma_5)]\}\mathfrak{N}(x_4)\\&\times iD_{\mu\nu}(x_1-x_4;m_W{}^2)\,iD_{\alpha\beta}(x_2-x_3;m_W{}^2)-(m_{\mathcal{P}}\to m_{\mathcal{P}'}))\,,\end{aligned} \tag{F3}$$

where the factor 4! in the expansion of the exponential is canceled by the number of ways ($\frac{1}{2}$4!) the Wick contradiction of $(\mathcal{L}_I)^4$ yields the term on the right-hand side of (F3). The integral implied in (F3) can best be evaluated in momentum space. The relevant integral is of the form

$$\int \frac{d^4k}{(2\pi)^4} \{\gamma^\alpha \not{k} \gamma^\beta [\tfrac{1}{2}(1-\gamma_5)]\} \{\gamma_\beta \not{k} \gamma_\alpha [\tfrac{1}{2}(1-\gamma_5)]\} \left(\frac{1}{k^2 - m_{\varphi}^2} - \frac{1}{k^2 - m_{\varphi'}^2} \right)^2 \frac{1}{(k^2 - m_W^2)^2}$$

$$\simeq \frac{-i}{16^2 m_W^2} \frac{\delta}{m_W^2} \{\gamma^\alpha [\tfrac{1}{2}(1-\gamma_5)]\} \{\gamma_\alpha [\tfrac{1}{2}(1-\gamma_5)]\} ,$$

where use of (C3) has been made, and

$$\delta \simeq m_{\varphi'}^2 \quad \text{if } m_W^2 \gg m_{\varphi'}^2 \gg m_\varphi^2$$
$$\simeq 2(m_{\varphi'} - m_\varphi)^2 \quad \text{if } m_W^2 \gg m_{\varphi'}^2 \simeq m_\varphi^2 . \qquad \text{(F4)}$$

In the local limit S_4 may be written as

$$S_4 = -i \frac{G_F}{\sqrt{2}} \frac{\alpha}{4\pi} \epsilon_0 \cos^2\theta_C \sin^2\theta_C \times \int d^4x \{\bar{\lambda}(x) \gamma_\mu [\tfrac{1}{2}(1-\gamma_5)] \mathfrak{N}(x)\}^2 ,$$

where

$$\epsilon_0 = \frac{\delta}{m_W^2 \sin^2\theta_W} = \frac{\delta}{(38\ \text{GeV})^2} . \qquad \text{(F5)}$$

Consequently the effective Lagrangian is

$$\mathcal{L}_{\text{eff}} = -\frac{G_F}{\sqrt{2}} \frac{\alpha}{4\pi} \epsilon_0 \cos^2\theta_C \sin^2\theta_C \times \{\bar{\lambda} \gamma_\mu [\tfrac{1}{2}(1-\gamma_5)] \mathfrak{N}\}^2 + \text{H.c.} \qquad \text{(F6)}$$

---

*On leave of absence from Laboratoire de Physique Théorique et Particules Elémentaires, Orsay (Laboratoire associé au CNRS), France.

†On leave of absence from the Institute for Theoretical Physics, State University of New York, Stony Brook, New York 11790.

‡Operated by Universities Research Association Inc. Under Contract with the United States Atomic Energy Commission.

[1] For a review of the subject up to September, 1972, see for example B. W. Lee, in *Proceedings of the XVI International Conference on High Energy Physics, Chicago-Batavia, Ill., 1972,* edited by J. D. Jackson and A. Roberts (NAL, Batavia, Ill., 1973), Vol. 4, p. 249; thereafter to September, 1973, see S. Weinberg, Rev. Mod. Phys. 46, 255 (1974).

[2] S. L. Glashow, J. Iliopoulos, and L. Maiani, Phys. Rev. D 2, 1285 (1970).

[3] S. Weinberg, Phys. Rev. Lett. 19, 1264 (1967); A. Salam, in *Elementary Particle Theory: Relativistic Groups and Analyticity (Nobel Symposium No. 8),* edited by N. Svartholm (Almqvist and Wiksell, Stockholm, 1968), p. 367. The scheme which incorporates hadrons is discussed in S. Weinberg, Phys. Rev. Lett. 27, 1688 (1971).

[4] H. Georgi and S. L. Glashow, Phys. Rev. Lett. 28, 1494 (1972).

[5] W. C. Carithers, D. R. Nygren, H. A. Gordon, M. L. Ioffredo, K.-W. Lai, and P. Weilhammer, Phys. Rev. Lett. 31, 1025 (1973): This paper gives the average branching ratio of $\Gamma(K_L \to \mu\bar{\mu})/\Gamma(K_L \to \text{all}) = (12^{+8}_{-4}) \times 10^{-9}$.

[6] The branching ratio for $K_L \to \gamma\gamma$ (see Table I) is taken from the Particle Data Group, Rev. Mod. Phys. 45, S1 (1973).

[7] For a review of this subject, see M. K. Gaillard and H. Stern, Ann. Phys. (N.Y.) 76, 580 (1973); A. D. Dolgov, L. B. Okun, and V. I. Zakharov, in *Neutrino '72,* proceedings of the Euro-Physics Conference, Balatonfüred, Hungary, 1972, edited by A. Frenkel and G. Marx (OMKDK-TECHOINFORM, Budapest, 1972), Vol. 1, p. 269.

[8] We wish to thank T. D. Lee for bringing this point to our attention.

[9] G. 't Hooft, Nucl. Phys. B35, 167 (1971): A general gauge formulation of spontaneously broken gauge theories is discussed by K. Fujikawa, B. W. Lee, and A. I. Sanda, Phys. Rev. D 6, 2923 (1972).

[10] D. Gross and F. Wilczek, Phys. Rev. D 8, 3633 (1973); S. Weinberg, Phys. Rev. Lett. 31, 494 (1973); H. Fritzsch, M. Gell-Mann, and H. Leutwyler, Phys. Lett. 47B, 365 (1973).

[11] A. Chodos, R. L. Jaffe, K. Johnson, C. B. Thorn, and V. F. Weisskopf, Phys. Rev. D 9, 3471 (1974).

[12] S. Weinberg, Phys. Rev. D 8, 605 (1973); 8, 4482 (1973).

[13] T. Appelquist, J. D. Bjorken, and M. Chanowitz, Phys. Rev. D 7, 2225 (1973).

[14] E. Ma, Phys. Rev. D 9, 3103 (1974).

[15] J. Smith and Z. Uy, Phys. Rev. D 7, 2738 (1973); F. Bogomolny *et al., ibid.* 8, 3237 (1973).

[16] G. Snow, Nucl. Phys. B55, 445 (1973); J. Rosner, unpublished work.

[17] See, for example, S. L. Adler and R. F. Dashen, *Current Algebra* (Benjamin, New York, 1968).

[18] C. G. Callan and S. B. Treiman, Phys. Rev. Lett. 16, 153 (1966); V. S. Mathur, S. Okubo, and L. K. Pandit, *ibid.* 16, 371 (1966).

[19] L. Rosenberg, Phys. Rev. 129, 2786 (1963); S. L. Adler, Phys. Rev. 117, 2426 (1969).

[20] B. R. Martin, E. de Raphael, and J. Smith, Phys. Rev. D 2, 179 (1970) and references cited therein. See also R. L. Goble, *ibid.* 7, 937 (1973); F. Y. Yndurain, Prog. Theor. Phys. 46, 990 (1971); Y. Kohara, *ibid.* 48, 261 (1972).

[21] See also J. Smith and Z. E. S. Uy, Phys. Rev. D 8, 3056 (1973).

[22] This is attributed to D. Cline, H. Haggerty, W. Single-

ton, W. Fry, and N. Schgal, paper submitted to the XVI International Conference on High Energy Physics, Chicago-Batavia, Illinois, 1972. A more detailed description of the experiment is available by Douglas B. Clark, Ph.D. thesis, Univ. of Wisconsin, 1973 (unpublished); this paper contains a very thorough review of theoretical work on $K^+ \to \pi^+ e\bar{e}$. Among the papers cited, the following are of particular interest to us, since the approaches of these papers are complementary to ours: M. A. B. Bég, Phys. Rev. 132, 426 (1963); V. V. Geidt and I. B. Khriplovich, Yad. Fiz. 8, 960 (1968) [Sov. J. Nucl. Phys. 8, 558 (1969)]. The unitarity contribution has been calculated by G. Segrè and D. Wilkinson, Phys. Rev. D 8, 3056 (1973) and is negligible.

[23]S. Gjesdal, G. Presser, P. Steffen, J. Steinberger, F. Vannucci, H. Wahl, H. Filthuth, K. Kleinknecht, V. Lüth, and G. Zech, Phys. Lett. 44B, 217 (1973).

[24]G. D. Cable, R. H. Hildebrand, C. Y. Pang, and R. Stiening, Phys. Rev. D 8, 3807 (1973).

[25]B. W. Lee, J. R. Primack, and S. B. Treiman, Phys. Rev. D 7, 510 (1973); B. W. Lee and S. B. Treiman, Phys. Rev. D 7, 1211 (1973).

[26]K. Fujikawa, B. W. Lee, and A. I. Sanda, Phys. Rev. D 6, 2923 (1972); J. R. Primack and H. Quinn, *ibid.* 6, 3171 (1972).

[27]I. Bars, M. B. Halpern, and M. Yoshimura, Phys. Rev. Lett. 29, 969 (1972); Phys. Rev. D 7, 1233 (1973).

[28]B. W. Lee, Phys. Rev. D 6, 1188 (1972); J. Prentki and B. Zumino, Nucl. Phys. B47, 99 (1972).

[29]B. W. Lee, Phys. Rev. D 9, 933 (1974).

[30]See for example, J. D. Bjorken and S. D. Drell, *Relativistic Quantum Mechanics* (McGraw-Hill, New York, 1964), Sec. 8.2.

PHYSICAL REVIEW D VOLUME 10, NUMBER 3 1 AUGUST 1974

$\eta'(958)$ branching ratio, linear matrix element, and dipion phase shift*

George R. Kalbfleisch
Brookhaven National Laboratory, Upton, New York 11973
(Received 28 February 1974)

The "world" data on $\eta'(958)$ in regard to the branching ratio $R = (\pi^+\pi^-\gamma/\pi^+\pi^-\eta_N)$, η_N denoting $\eta(549) \to$ all neutrals, and the dipion mass spectrum in the $\eta' \to \pi^+\pi^-\eta$ decay are reviewed. We find that $R = 0.97 \pm 0.08$ independent of energy, exclusive of the data of Aguilar-Benitez *et al.* Under the assumption that $J^P = 0^-$, the best value of the α parameter of the linear matrix element is $\alpha = -0.08 \pm 0.03$. Possible connections between the dipion mass spectrum and δ_{00}, the $I = J = 0$ phase shift, are discussed.

Many studies of the $\eta'(958)$ have been made. We comment here on the branching ratio $R = (\pi^+\pi^-\gamma/\pi^+\pi^-\eta_N)$, where η_N represents $\eta(549) \to$ all neutrals, and on the linear matrix element of the $\eta'(958)$. We base these comments on the data presented in Refs. 1–6; some additional data are not used.[7] We obtain the current "world" averages of R and of α, the parameter characterizing the linear matrix element. We also comment on possible connections with δ_{00}, the $I = J = 0$ dipion phase shift. Additional comments on the $\eta'(958)$ are given in Ref. 8.

BRANCHING RATIO

The data of Refs. 1–6 on the branching ratio $R = (\pi^+\pi^-\gamma/\pi^+\pi^-\eta_N)$ are given in Table I and are shown in Fig. 1 versus the momentum of the incident beam in the experiments. Included is the branching ratio of the $M(953)$ of Ref. 3. The values of the η' branching ratio R from Refs. 1, 2, and 4–6 are consistent; the weighted average is $\bar{R} = 0.97 \pm 0.08$ and is indicated also in Fig. 1. The value of R for the $\eta'(958)$ from Ref. 3 is in disagreement with this average value. Since there is no evidence that the $\pi^+\pi^-\gamma$ and $\pi^+\pi^-\eta$ states at 958 MeV are different,[5] we must attribute the disagreement between $\bar{R}$ and R (Ref. 3) to some unknown systematic effect in that experiment. The evidence that the $M(953)$ is not identical to $\eta'(958)$ rests in the $M(\pi^+\pi^-)$ distribution of the $\pi^+\pi^-\gamma$ decay mode. The data in the ρ^0 region of both the $\eta'(958)$ and $M(953)$ data samples have the characteristic $\sin^2\theta_{\pi^+\gamma}$ distribution of $\eta'(958)$ events.[3] Therefore, the evidence for an $M(953)$ should be obtained from the $M(\pi^+\pi^-)$ mass distribution, Fig. 46(a) of Ref. 3, where events containing a $\rho^0(765)$ were excluded. The data yield 37 ± 10 events outside the ρ band, of which about 8–15 should be attributed to the tail of the ρ^0 in $\eta' \to \rho^0\gamma$ decay. Thus, the evidence for an $M(953)$ is about 2 to 3 standard deviations, attributing all the other "M" events to $\eta'(958)$; then the branching ratio R of the η' in the "M" sample is about 0.8 ± 0.2.